

# Membrane-bound structure and energetics of $\alpha$ -synuclein

Maja Mihajlovic and Themis Lazaridis\*

Department of Chemistry, City College of New York, CUNY, New York, New York 10031

## ABSTRACT

Aggregation and fibrillation of  $\alpha$ -synuclein bound to membranes are believed to be involved in Parkinson's and other neurodegenerative diseases. On SDS micelles, the N-terminus of  $\alpha$ -synuclein forms two curved helices linked by a short loop. However, its structure on lipid bilayers has not been experimentally resolved. Using MD simulations with an implicit membrane model we show here that, on a planar mixed membrane, the truncated  $\alpha$ -synuclein (residues 1–95) forms a bent helix. Bending of the helix is not due to the protein sequence or membrane binding, but to collective motions of the long helix. The backbone of the helix is  $\sim 2.5$  Å above the membrane surface, with some residues partially inserted in the membrane core. The helix periodicity is 11/3 (11 residues complete three full turns) as opposed to 18/5 periodicity of an ideal  $\alpha$ -helix, with hydrophobic residues towards the membrane, negatively charged residues towards the solvent and lysines on the polar/nonpolar interface. A series of threonines, which are characteristic for  $\alpha$ -synuclein and perhaps a phosphorylation site, is also located at the hydrophobic/hydrophilic interface with their side chain often hydrogen bonded to the main-chain atom. The calculations show that the energy penalty for change in periodicity from the 18/5 to 11/3 on the anionic membrane is overcome by favorable solvation energy. The binding of truncated  $\alpha$ -synuclein to membranes is weak. It prefers anionic membranes but it also binds marginally to a neutral membrane, via its C-terminus. Dimerization of helical monomers on the mixed membrane is energetically favorable. However, it slightly interferes with membrane binding. This might promote lateral diffusion of the protein on the membrane surface and facilitate assembly of oligomers that precede fibrillation.

Proteins 2008; 70:761–778.  
© 2007 Wiley-Liss, Inc.

**Key words:** molecular dynamics simulation; implicit membrane; helix bending; 11/3 periodicity; 11-residue repeat; coiled-coil.

## INTRODUCTION

$\alpha$ -Synuclein is a small presynaptic protein that belongs to the same protein family as  $\beta$ -synuclein and  $\gamma$ -synuclein.<sup>1,2</sup> It is commonly believed to play a role in diseases such as Parkinson's disease (PD),<sup>3,4</sup> Alzheimer's disease (AD),<sup>5</sup> Down's syndrome,<sup>6</sup> and Hallervorden-Spatz syndrome.<sup>7</sup> For instance, a large population of  $\alpha$ -synuclein is found in Lewy body filaments that are a distinctive pathological characteristic of PD and dementia with Lewy bodies.<sup>3,4</sup> Three missense mutations, A30P,<sup>8</sup> E46K,<sup>9</sup> and A53T,<sup>10</sup> are related to familial PD.  $\alpha$ -Synuclein is postulated to serve as a fatty acid binding protein<sup>11</sup> and likely has a role in a fatty acid uptake and metabolism.<sup>12</sup> In songbird brain, it may be involved in the song control circuit during the song learning period, through modulating synaptic plasticity.<sup>13</sup> It has also been reported that  $\alpha$ -synuclein inhibits phospholipase D2,<sup>14,15</sup> determines the size of vesicular pool<sup>16,17</sup> or not,<sup>18,19</sup> influences the level of dopamine,<sup>18–20</sup> complexins, and 14-3-3 proteins,<sup>19</sup> and repairs neurodegeneration in mice produced by deletion of cystein-string protein- $\alpha$  that inhibits assembly of the SNARE complex.<sup>21</sup>

As other synucleins,  $\alpha$ -synuclein is unstructured in solution. Binding to anionic membranes induces folding of its N-terminus into an amphipathic helix, whereas the C-terminus (residues  $\sim 98$ –140) remains unstructured.<sup>22–26</sup> The helical content is much lower in buffer and in the presence of zwitterionic membranes.<sup>22,27</sup> Binding of  $\alpha$ -synuclein seems to be lipid specific and dependent on vesicle size.<sup>22,27–31</sup> On the basis of available data, it is not clear whether  $\alpha$ -synuclein binds to zwitterionic membranes. Several groups reported that the presence of anionic lipids is necessary for binding of  $\alpha$ -synuclein to membranes,<sup>22,24,30</sup> whereas others observed binding of wild-type  $\alpha$ -synuclein or of the truncated protein (residues 1–95) to zwitterionic lipids.<sup>31–35</sup> In solution,  $\alpha$ -synuclein has a propensity to

*Abbreviations:* AD, Alzheimer's disease; elec, electrostatic energy; GC, Gouy-Chapman energy; LUV, large unilamellar vesicle; MD, molecular dynamics; NAC, non-A $\beta$  component of AD amyloid; NOE, nuclear overhauser effect; PD, Parkinson's disease; SDS, sodium dodecyl sulfate; solv, solvation free energy; SUV, small unilamellar vesicle; vdW, van der Waals energy.

The Supplementary Material referred to in this article can be found online at <http://www.interscience.wiley.com/jpages/0887-3585/suppmat>.

Grant sponsor: National Science Foundation; Grant number: MCB-0316667; Grant sponsor: NIH (RCMI grant); Grant number: RR03060.

\*Correspondence to: Themis Lazaridis, Department of Chemistry, City College of New York, CUNY, 138th Street and Convent Avenue, New York, NY 10031. E-mail: [tlazaridis@ccny.cuny.edu](mailto:tlazaridis@ccny.cuny.edu)

Received 28 February 2006; Revised 3 April 2007; Accepted 11 April 2007

Published online 29 August 2007 in Wiley InterScience (www.interscience.wiley.com).

DOI: 10.1002/prot.21558

aggregate, in a nucleation-dependent manner, and afterwards to form  $\beta$ -sheet rich fibrils.<sup>36</sup> Fibrils and/or protofibrils are believed to be neurotoxic.<sup>37–39</sup>

The sequence of  $\alpha$ -synuclein consists of 140 amino acids. Similarly to the exchangeable apolipoproteins<sup>40,41</sup> and phosphocholine cytidyltransferase,<sup>42,43</sup> the N-terminus of  $\alpha$ -synuclein contains seven imperfect 11-residue repeats (Fig. 1), with the sixth repeat lacking the consensus motif KAKEGV or KTKEGV. Related to its 11-residue repeat sequence and a propensity to form a curved amphipathic helix that wraps around lipid particles, Segrest *et al.* proposed that the helix of apolipoprotein A-I is an  $\alpha$ 11/3 helix, which has 3.67 residues per turn instead of 3.6 residues per turn of an ideal  $\alpha$ -helix.<sup>44</sup> It has been established that the same periodicity exists in repeats 5–7 of  $\alpha$ -synuclein bound to SUVs<sup>45</sup> as well as in  $\alpha$ -synuclein bound to micelles.<sup>46</sup> The region enclosed by residues 61–95, the so-called non-A $\beta$  component of AD amyloid (NAC) region,<sup>5</sup> seems to be prone to fibrillation. Giasson *et al.* noted that the peptide corresponding to residues 71–82 of  $\alpha$ -synuclein forms fibrils and initiates aggregation of wild-type  $\alpha$ -synuclein.<sup>47</sup>  $\beta$ -Synuclein lacks 11 residues in the NAC region, whereas the sequence of  $\gamma$ -synuclein largely diverges from the sequence of the NAC in  $\alpha$ -synuclein; these synucleins are not found in Lewy bodies<sup>4</sup> and have a reduced tendency to form fibrils.<sup>48,49</sup>

The structure of monomeric  $\alpha$ -synuclein bound to SDS micelles has been determined using nuclear magnetic resonance (NMR) spectroscopy.<sup>24–26,50</sup> The N-terminal  $\alpha$ -helix (residues 1–94) is broken into two curved helices, connected by a short linker involving residues ~42–44. The structure of  $\alpha$ -synuclein bound to vesicles is unknown, although there are indications that it is either similar to that on SDS micelles<sup>24</sup> or a continuous helix.<sup>23,45</sup>

Oligomerization of  $\alpha$ -synuclein on vesicles or micelles is also a point of debate. Dimers were produced by incubation of  $\alpha$ -synuclein with PI (phosphatidylinositol) containing vesicles,<sup>22</sup> or PIP<sub>2</sub> (phosphatidylinositol 4,5-bisphosphate) vesicles or in the presence of long chain polyunsaturated fatty acids.<sup>51</sup>  $\alpha$ -Synuclein oligomers (~45 kDa, the molecular mass of monomeric  $\alpha$ -synuclein is ~17 kDa), exclusively bound to lipid membranes, were isolated from human dopaminergic cells SH-SY5Y.<sup>52</sup> It has been reported that, under nonreducing conditions,  $\alpha$ -synuclein forms helical dimers in the presence of bPE

(brain L- $\alpha$ -phosphatidylethanolamine)/bPS (brain L- $\alpha$ -phosphatidylserine) MLVs (multilamellar vesicles)<sup>53</sup> and that lipid vesicles promote fibrillation of wild type  $\alpha$ -synuclein.<sup>54</sup> In the presence of synthetic cross-linking reagents, Cole *et al.* detected dimers and trimers that preferentially bind to lipid droplets, though they did not determine the conformation of oligomers.<sup>55</sup> Lee *et al.* found that the membrane-bound  $\alpha$ -synuclein has a high propensity to aggregate and to seed the aggregation of its soluble form.<sup>56</sup> Necula *et al.* also observed that anionic micelles and vesicles could induce  $\alpha$ -synuclein fibrillation.<sup>57</sup> A recent MD study showed that  $\alpha$ -synuclein, modeled using the micelle-bound NMR structure as the initial structure and docked on a flat surface, forms dimers as well as pentamers and hexamers that form ring-like structures.<sup>58</sup> However, Narayanan and Scarlata showed that increased protein concentration promotes self-association of the protein, but the effect was inhibited by increased concentration of lipids.<sup>32</sup> In addition, Zhu and Fink reported that the helical conformation on its own inhibits aggregation.<sup>29</sup> A recent paper by Ahmad *et al.* argues that the formation of fibrils in the presence of SDS micelles depends on detergent concentration: at SDS concentration below 2 mM,  $\alpha$ -synuclein is partially folded and capable of making fibrils; at larger SDS concentrations,  $\alpha$ -synuclein is fully folded (i.e., helical) and does not make fibrils.<sup>59</sup>

The goal of the present study was to determine the structure of the N-terminal domain of  $\alpha$ -synuclein on planar anionic membranes using theoretical methods. We also explore the ability of  $\alpha$ -synuclein to bind planar membranes composed of zwitterionic lipids and the viability of protein dimerization on the mixed membrane. Taking advantage of readily available energy components calculated from MD trajectories, we quantify the energetics of membrane binding, change in helix periodicity, and dimerization.

## METHODS

### Implicit membrane model

Molecular dynamics simulations were carried out using the program CHARMM.<sup>60</sup> The effective energy of a solute is calculated using an implicit model, IMM1-GC<sup>61</sup> on anionic membranes and IMM1<sup>62</sup> on neutral membranes.

MDVFMKGLSKAKEGVVAAA**E**KT**K**QGVAA**E**AAGKTKEGVLYV**G**SK**T**KEGVV  
 HGVATVA**E**KTKEQVTNV**G**GAV**V**T**G**VTA**V**AQ**K**TVEGAGSIAA**T**GFV

**Figure 1**

The amino acid sequence of the first 95 residues of  $\alpha$ -synuclein. The six 11-residue repeats containing the consensus motif KAKEGV or KTKEGV (shown in bold letters) are colored in gray and shown in alternating roman and italic print for easier reading. The 11-residue repeat without the consensus motif is shown in underlined italic.

The effective energy equals the sum of the intramolecular energy of the solute,<sup>63</sup> the solvation free energy accounting for interactions of each atom with solvent, and, in the case of anionic membranes, the lipid headgroup-solute electrostatic interaction energy, obtained from the Gouy-Chapman theory for the electrical double layer.<sup>64</sup>

### Simulation protocols

The membrane is taken to be parallel to the  $xy$ -plane, with its center located at  $z = 0$ . The hydrocarbon core of the membrane was 23 Å wide. The hydrophobic/hydrophilic interface is thus at  $z = \pm 11.5$  Å and the plane of smeared charges, corresponding to the position of phosphates, is at  $z = \pm 14.5$  Å. Henceforth, a position mentioned in the text refers to the  $z$ -coordinate. The valence of anionic lipids was 1, with area 70 Å<sup>2</sup> per lipid. As in experiment, the mixed membrane consisted of 30 mol % of anionic lipids at 0.02M salt and the temperature was 298 K.<sup>24</sup> All energy minimizations were done using the adopted basis Newton-Raphson algorithm (ABNR). The numerical integration of equations of motion was carried out using the Verlet integrator with a time step of 2 fs. All bonds involving hydrogen atoms were fixed using SHAKE constraints. Unless otherwise noted, error bars are the standard deviation of the mean.

### Initial structures

Since experiment has already shown that the membrane-bound N-terminal domain of  $\alpha$ -synuclein (residues 1 through 95) is helical,<sup>22–26</sup> we start the simulations from an ideal  $\alpha$ -helix ( $\phi_i = -57^\circ$ ,  $\psi_i = -47^\circ$ ). Figure 1 shows the amino acid sequence of the protein. A dimer was built by placing two monomers on the membrane surface, parallel or antiparallel to each other, with their center of mass 15 Å apart.

We previously reported that the protonation of glutamates is a prerequisite for binding of the helical peptide VEEKS, derived from the membrane-binding domain of phosphocholine cytidyltransferase,<sup>43</sup> to anionic membranes.<sup>65</sup> VEEKS is similar to  $\alpha$ -synuclein in that it consists of three 11-residue repeats, forms an amphipathic helix on anionic membranes, its lysine residues are at the polar/nonpolar interface and are key to binding, and its polar face is rich in glutamates and aspartates. However, three glutamates of VEEKS are located on the polar/nonpolar interface and their protonation state controls pH-dependent binding of the protein to anionic membranes. In the truncated  $\alpha$ -synuclein, all lysines are at the polar/nonpolar interface and all glutamates and an aspartate are in the polar face of the helix, as is typical for class A helices.<sup>40</sup> Therefore, we deem that their ionization state does not interfere with the binding, at least not to a large extent, and that, at pH around 7, all acidic residues are deprotonated and His is protonated.

### Determination of the optimal orientation

Four simulations were run starting from an ideal  $\alpha$ -helix at four arbitrary orientations, obtained by rotating the protein 90° around the  $x$ -axis. The center of the protein and the center of the membrane were first aligned with the  $x$ -axis. The protein, in each of the four orientations, was then placed on the membrane surface (its center of mass at 17 Å) and its energy was minimized, followed by a 12-ns MD simulation. All simulations were run using four sets of random numbers, and the energies were averaged over the four seeds. The average energy was compared with the energies of the structures obtained from the other three simulations; the optimal orientation relative to the membrane corresponded to that which yielded the lowest average energy.

In the case of a dimer, the initial orientation of each monomer, relative to the membrane, was the same as that which resulted in the optimal orientation of the monomer. Three sets of 12-ns MD simulations were performed: (1) on the parallel dimer, (2) on the antiparallel dimer, and (3) on two mutually noninteracting monomers. All simulations were repeated using three additional seeds. The energies were averaged over the last 11 ns of each simulation and then over the four seeds. Whether the parallel or the antiparallel dimer is more favorable is determined based on the lower average energy.

To calculate the average water-to-membrane transfer energy, effective energies were extracted from MD trajectories, saved every 2 ps, and averaged over the last 11 ns. The energy of the protein in solvent was obtained by transferring the protein from the membrane to solvent, at each frame, keeping the conformation the same to minimize statistical error. Again, the energies were averaged over the four seeds.

## RESULTS

### $\alpha$ -Synuclein on a neutral membrane

Several studies agree that  $\alpha$ -synuclein preferentially binds to anionic membranes as opposed to neutral membranes.<sup>22,24,30</sup> However, Narayanan and Scarlata<sup>32</sup> and Rhoades *et al.*<sup>35</sup> observed that  $\alpha$ -synuclein also binds to LUVs composed of POPC (1-palmitoyl-2-oleoyl-*sn*-glycero-3-phosphocholine). Nuscher *et al.*<sup>31</sup> and Kamp and Beyer<sup>34</sup> reported binding of wild-type  $\alpha$ -synuclein to SUVs composed of DMPC (1,2-dimyristoyl-*sn*-glycero-3-phosphocholine) or of DPPC (1,2-dipalmitoyl-*sn*-glycero-3-phosphocholine) in the gel phase, but neither to SUVs in the liquid crystalline state nor to LUVs. A recent paper by Ramakrishnan *et al.* suggests that, although wild-type  $\alpha$ -synuclein does not bind, the truncated  $\alpha$ -synuclein (residues 1–95) binds to DMPC membranes over a broad temperature range.<sup>33</sup> Motivated by these contradictory

findings, we tested whether the truncated  $\alpha$ -synuclein binds to neutral membranes equivalent to DMPC bilayers.

Sixteen 12-ns MD simulations were performed to test binding of the truncated  $\alpha$ -synuclein to the neutral membrane, exploring the four orientations of the protein relative to the membrane, each orientation tested using four random numbers to initialize velocities. In 7 out of the 16 simulations, the protein binds to the membrane for at least  $\sim 3.5$  ns and at most  $\sim 10$  ns. If binding takes place, regardless of the initial orientation, the protein quickly reorients at the beginning of the simulation to essentially the same orientation relative to the membrane (i.e., with the hydrophobic face of the helix next to the membrane and the hydrophilic face exposed to solvent). To compare energies of all membrane-bound conformations (generated in the seven simulations), the energies were averaged between 1 and 3.5 ns, time period during which binding takes place in all the simulations. The average energies obtained from 6 out of the 7 simulations differ by no more than 5 kcal/mol whereas that from the seventh simulation is  $\sim 17$  kcal/mol higher than the lowest average energy. The energy of the protein, averaged over all seven simulations, is  $\sim 6$  kcal/mol lower than the same conformation in water, due to favorable hydrophobic

interactions (Table I). Although the protein moves away from the membrane in long simulations, we consider both the structure and the water-to-membrane transfer energy when deciding whether the protein binds to the membrane. In the case of nonconstitutive binding to membranes, unconstrained simulations will always lead to unbinding at some point due to entropic reasons.

Figure 2 shows snapshots of the truncated  $\alpha$ -synuclein on the neutral membrane from the 12-ns MD simulation that yields the lowest energy and during which the protein stays bound to the membrane up to  $\sim 10$  ns. The somewhat destabilized N-terminal half of the helix is detached from the membrane surface, which is not surprising given the number of charged residues and the propensity of the helix to unravel in solvent. As the snapshots suggest, this domain is very flexible; during the simulation it flips about relative to the membrane-bound C-terminus. Membrane binding is facilitated by the hydrophobic residues that slightly insert in the membrane core.

### $\alpha$ -Synuclein on a mixed membrane

Regardless of the initial orientation, the helix reorients at the onset of the MD simulations so that hydrophobic

**Table I**  
Average Effective Energies (in kcal/mol) of the Truncated  $\alpha$ -Synuclein on Membranes

	Neutral membrane <sup>a</sup>	Mixed membrane <sup>b</sup>	Dimer on mixed membrane <sup>c</sup>
$\langle W \rangle_{\text{mem}}^{\text{d}}$	$-1977.24 \pm 1.23$	$-1990.54 \pm 0.47$ $-1987.38 \pm 0.45$ $-1985.13 \pm 0.45$ $-1984.42 \pm 0.51$	$-4024.67 \pm 0.63$ $-3996.92 \pm 0.65$ $-3964.73 \pm 0.66$
$\langle \Delta W \rangle = W_{\text{mem}} - W_{\text{water}}^{\text{e}}$	$-5.85 \pm 1.74^{\text{f}}$	$-11.53 \pm 0.66^{\text{g}}$ $-11.01 \pm 0.63^{\text{h}}$ $-9.30 \pm 0.64^{\text{k}}$ $-10.08 \pm 0.72^{\text{m}}$	$-16.03 \pm 0.88^{\text{h}}$ $-17.33 \pm 0.91^{\text{j}}$ $-19.88 \pm 0.92^{\text{l}}$
$\langle \text{GC} \rangle^{\text{n}}$		$-8.69 \pm 0.04$ $-8.63 \pm 0.04$ $-7.99 \pm 0.04$ $-8.12 \pm 0.04$	$-13.89 \pm 0.05$ $-15.44 \pm 0.05$ $-16.96 \pm 0.07$

<sup>a</sup>Averages are calculated between 1 ns and 3.5 ns of 7 MD simulations started from different initial orientation of the protein relative to the membrane and run using four seeds.

<sup>b</sup>Averages are calculated over the last 11 ns of 12-ns MD simulations performed using four seeds. The four values correspond to the four initial orientations of the protein.

<sup>c</sup>Averages are calculated over the last 11 ns of 12-ns MD simulations and four seeds. The first value corresponds to an antiparallel dimer, the second value corresponds to a parallel dimer and the third value corresponds to two non-interacting monomers.

<sup>d</sup>Error bars are the standard deviation of the mean.

<sup>e</sup>The average effective energy of the protein on a membrane.

<sup>f</sup>The average effective transfer energy calculated as the difference between the average effective energy of the protein on a membrane and in water ( $W_{\text{water}}$ ).

<sup>g</sup> $\langle \Delta W_{\text{elec}} \rangle = -8.63 \pm 1.76$ ;  $\langle \Delta W_{\text{solv}} \rangle = 2.78 \pm 0.94$ ;  $\langle \Delta W_{\text{polar}} \rangle = 20.58 \pm 1.13$ ;  $\langle \Delta W_{\text{alip}} \rangle = -17.32 \pm 0.39$ ;  $\langle \Delta W_{\text{arom}} \rangle = -0.48 \pm 0.04$ , where "elec" denotes the electrostatic energy, "solv" is the total solvation energy, and "polar," "alip," and "arom" are components of the solvation energy due to polar, aliphatic, and aromatic groups, respectively.

<sup>h</sup> $\langle \Delta W_{\text{elec}} \rangle = -4.98 \pm 0.69$ ;  $\langle \Delta W_{\text{solv}} \rangle = 2.14 \pm 0.40$ ;  $\langle \Delta W_{\text{polar}} \rangle = 14.56 \pm 0.46$ ;  $\langle \Delta W_{\text{alip}} \rangle = -11.06 \pm 0.26$ ;  $\langle \Delta W_{\text{arom}} \rangle = -1.36 \pm 0.02$ .

<sup>i</sup> $\langle \Delta W_{\text{elec}} \rangle = -6.62 \pm 0.98$ ;  $\langle \Delta W_{\text{solv}} \rangle = 4.49 \pm 0.59$ ;  $\langle \Delta W_{\text{polar}} \rangle = 19.11 \pm 0.74$ ;  $\langle \Delta W_{\text{alip}} \rangle = -13.99 \pm 0.25$ ;  $\langle \Delta W_{\text{arom}} \rangle = -0.63 \pm 0.03$ .

<sup>j</sup> $\langle \Delta W_{\text{elec}} \rangle = -4.11 \pm 0.68$ ;  $\langle \Delta W_{\text{solv}} \rangle = 1.74 \pm 0.33$ ;  $\langle \Delta W_{\text{polar}} \rangle = 12.35 \pm 0.43$ ;  $\langle \Delta W_{\text{alip}} \rangle = -9.32 \pm 0.22$ ;  $\langle \Delta W_{\text{arom}} \rangle = -1.30 \pm 0.02$ .

<sup>k</sup> $\langle \Delta W_{\text{elec}} \rangle = -4.24 \pm 0.89$ ;  $\langle \Delta W_{\text{solv}} \rangle = 2.34 \pm 0.60$ ;  $\langle \Delta W_{\text{polar}} \rangle = 14.01 \pm 0.72$ ;  $\langle \Delta W_{\text{alip}} \rangle = -10.13 \pm 0.21$ ;  $\langle \Delta W_{\text{arom}} \rangle = -1.54 \pm 0.03$ .

<sup>l</sup> $\langle \Delta W_{\text{elec}} \rangle = -2.66 \pm 0.63$ ;  $\langle \Delta W_{\text{solv}} \rangle = 1.34 \pm 0.39$ ;  $\langle \Delta W_{\text{polar}} \rangle = 8.49 \pm 0.44$ ;  $\langle \Delta W_{\text{alip}} \rangle = -5.93 \pm 0.11$ ;  $\langle \Delta W_{\text{arom}} \rangle = -1.21 \pm 0.02$ .

<sup>m</sup> $\langle \Delta W_{\text{elec}} \rangle = -5.77 \pm 1.02$ ;  $\langle \Delta W_{\text{solv}} \rangle = 2.85 \pm 0.53$ ;  $\langle \Delta W_{\text{polar}} \rangle = 18.64 \pm 0.63$ ;  $\langle \Delta W_{\text{alip}} \rangle = -13.57 \pm 0.28$ ;  $\langle \Delta W_{\text{arom}} \rangle = -2.22 \pm 0.03$ .

<sup>n</sup> $\langle \Delta W_{\text{elec}} \rangle = -3.81 \pm 0.82$ ;  $\langle \Delta W_{\text{solv}} \rangle = 1.85 \pm 0.48$ ;  $\langle \Delta W_{\text{polar}} \rangle = 11.25 \pm 0.57$ ;  $\langle \Delta W_{\text{alip}} \rangle = -8.44 \pm 0.23$ ;  $\langle \Delta W_{\text{arom}} \rangle = -0.96 \pm 0.02$ .

<sup>o</sup>The average Gouy-Chapman energy.

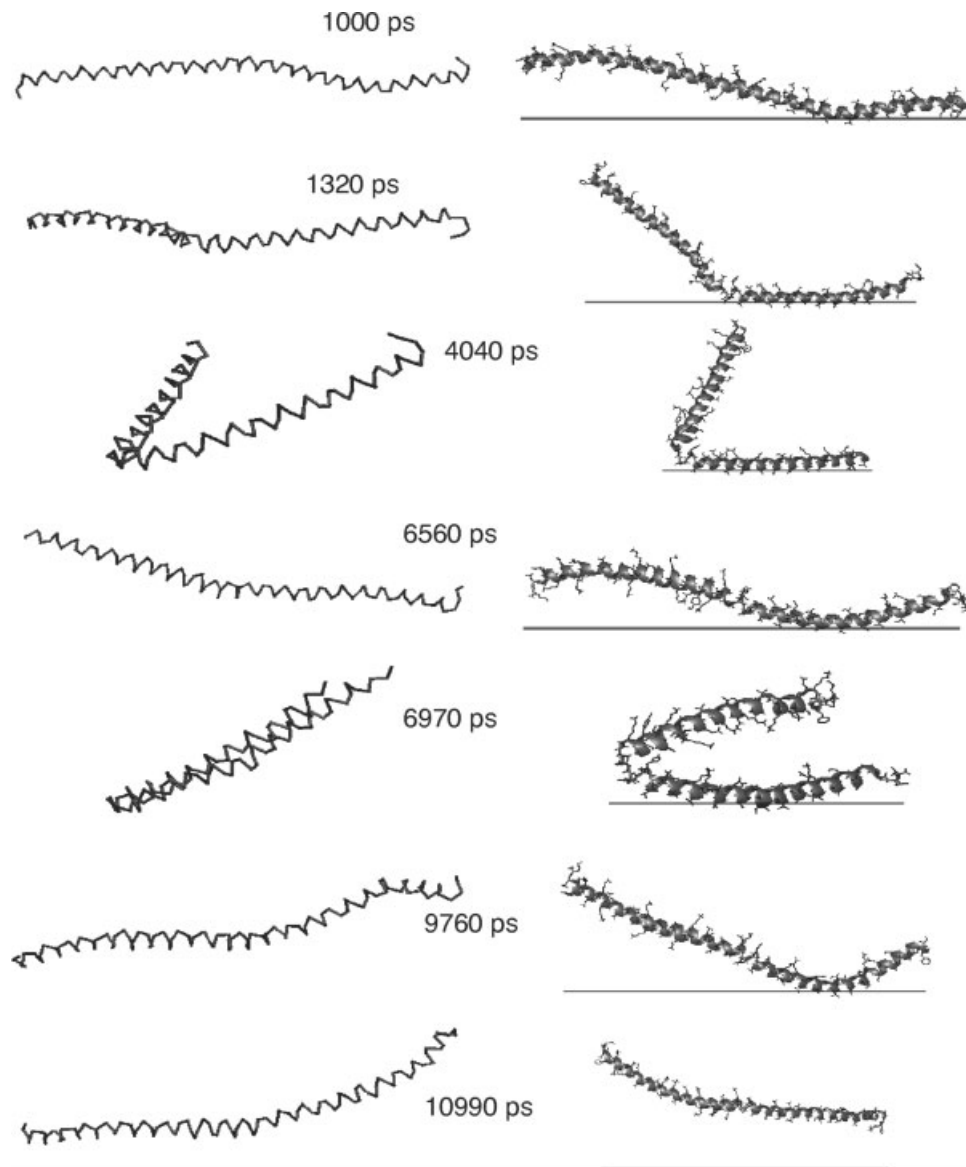


**Figure 2**

Snapshots of the truncated  $\alpha$ -synuclein on a neutral membrane from a MD trajectory. The line represents the hydrophobic/hydrophilic interface ( $z = 11.5 \text{ \AA}$ ). On the left is a view from above the membrane (shown are the  $C_{\alpha}$  atoms only) and on the right is a side view.

residues point towards the membrane surface, lysines are at the interface and acidic residues are in solvent. As a result, the average effective energy of the four runs is almost the same (the difference is not larger than 6 kcal/mol, as shown in Table I). On the basis of the average energies, binding is mainly due to favorable electrostatic interactions between the protein and the negative charge on the headgroups (see the  $\langle GC \rangle$  term in Table I), with a small contribution from hydrophobic interactions.

Figure 3(A) shows snapshots from a 12-ns MD simulation of  $\alpha$ -synuclein on the membrane containing 30 mol %

of anionic lipids, at 0.02M salt. The snapshots show that the truncated  $\alpha$ -synuclein is helical on the mixed membrane. Up to  $\sim 6.57$  ns, the entire helix interacts with the membrane, with occasional detachment of the C-terminus or, less frequently, of the N-terminus. Its center of mass is at  $\sim 17 \text{ \AA}$ , around  $2.5 \text{ \AA}$  above the phosphates (i.e., the plane of smeared charges). At later times, the C-terminus of the helix moves away from the membrane surface whereas the N-terminus interacts with the membrane until the end of the simulation. The effective energy of  $\alpha$ -synuclein on the mixed membrane calculated

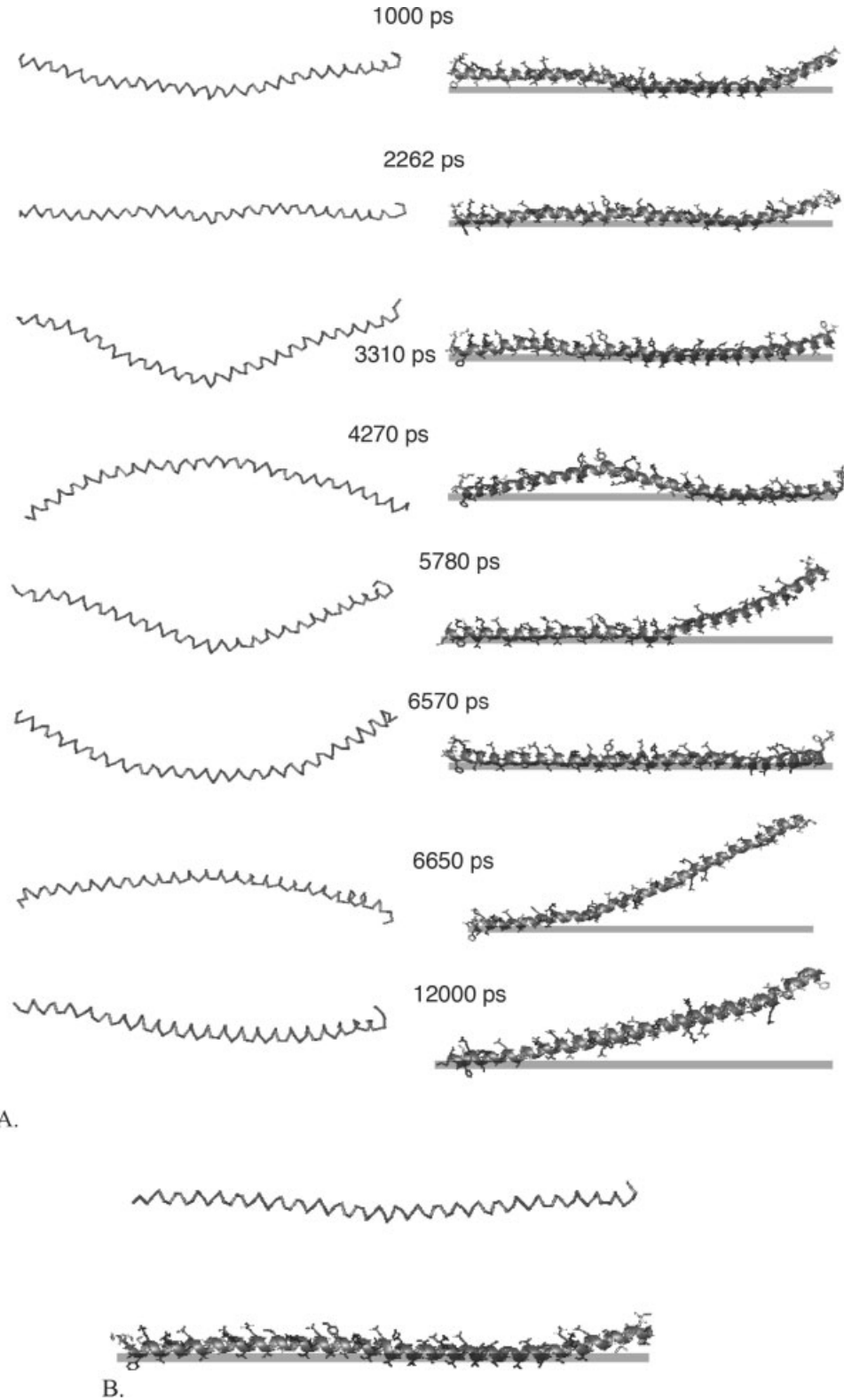


### Figure 3

The optimal orientation of the truncated  $\alpha$ -synuclein on the membrane containing 30 mol % of anionic lipids, at 0.02M salt concentration. **A:** Snapshots from a 12-ns MD simulation, viewed above the membrane (on the left) and from the side (on the right). **B:** The minimized average conformation, between 1 and 6.57 ns, viewed above the membrane (the upper figure) and from the side (the lower figure). The lower surface of the colored area represents the hydrophobic tail/headgroup interface ( $z = 11.5 \text{ \AA}$ ) and the upper surface corresponds to the plane of smeared charges ( $z = 14.5 \text{ \AA}$ ). In the snapshots taken above the membrane, only the  $C_{\alpha}$  atoms are depicted.

as a function of time shows a slight increase when the C-terminus of the helix detaches from the membrane (shown in Fig. S1 of the supplementary material section). A similar scenario has been observed in all simulations, though in a few of them the helix folds over so that its termini interact.

The helix shown in Figure 3(A) is bent. The bending angles between two local helix axes, defined by four consecutive  $C_\alpha$  atoms, were calculated using the HELANAL program<sup>66</sup> and the angles were averaged between 1 and 6.57 ns. The bending angle of  $0^\circ$  corresponds to completely straight helices. The local average bending angles at the intersecting residue are shown in Figure 4(A) (error bars are the standard deviation). Although the largest bending angle is at residue 47 ( $17.22^\circ \pm 8.35^\circ$ ), the bending is dispersed along the entire helix. The large standard deviations as well as the time evolution of the angle at residue 47, shown in Figure 4(B), suggest that the bending angles are not static but constantly undergo changes.

As Figure 4(C) illustrates, the average values of dihedral angles  $\phi_i$  and  $\psi_i$ , calculated between 1 and 6.57 ns of a MD simulation, are near their canonical values ( $\phi_i = -62^\circ$  and  $\psi_i = -41^\circ$ ), with the largest deviations in the terminal residues and E46 and G47 located in the

middle of the helix. Fluctuations of the dihedral angles are  $\sim 10^\circ$ , except at the N-terminus, G36, and in the middle of the helix [Fig. 4(D)]. Taken together, these data suggest that, due to bending motions (see below), the helix is most severely disturbed in its midsection, accompanied by a local co-operativity of neighboring dihedrals.

Another characteristic of an  $\alpha$ -helix is hydrogen bonds between backbone atoms. Figure 5 shows the average interaction energies between the backbone  $O_i$  atom and the backbone  $H_{i+4}$ ,  $H_{i+3}$ , or  $H_{i+5}$  atom, where averages are calculated between 1 and 6.57 ns of a 12-ns MD simulation. The  $O_i \dots H_{i+4}$  hydrogen bonds are dominant, though some residues occasionally make  $O_i \dots H_{i+3}$  or  $O_i \dots H_{i+5}$  hydrogen bonds, implying that the  $\alpha$ -helical conformation of the protein is preserved during the simulation, with some instabilities.

The  $O_i \dots H_{i+4}$  hydrogen bonds are perturbed about residues 43–47. Besides being hydrogen bonded to the H of G47, the O of K43 is sometimes hydrogen bonded to the H of V48 (the interaction energy of the former is  $-2.02 \pm 0.04$  kcal/mol and that of the latter is  $-0.13 \pm 0.02$  kcal/mol). The O of T44 is hydrogen bonded to the H of V48 ( $-2.02 \pm 0.04$  kcal/mol), to the H of V49 ( $-1.69 \pm 0.06$  kcal/mol) and to the H of G47 ( $-0.16 \pm$

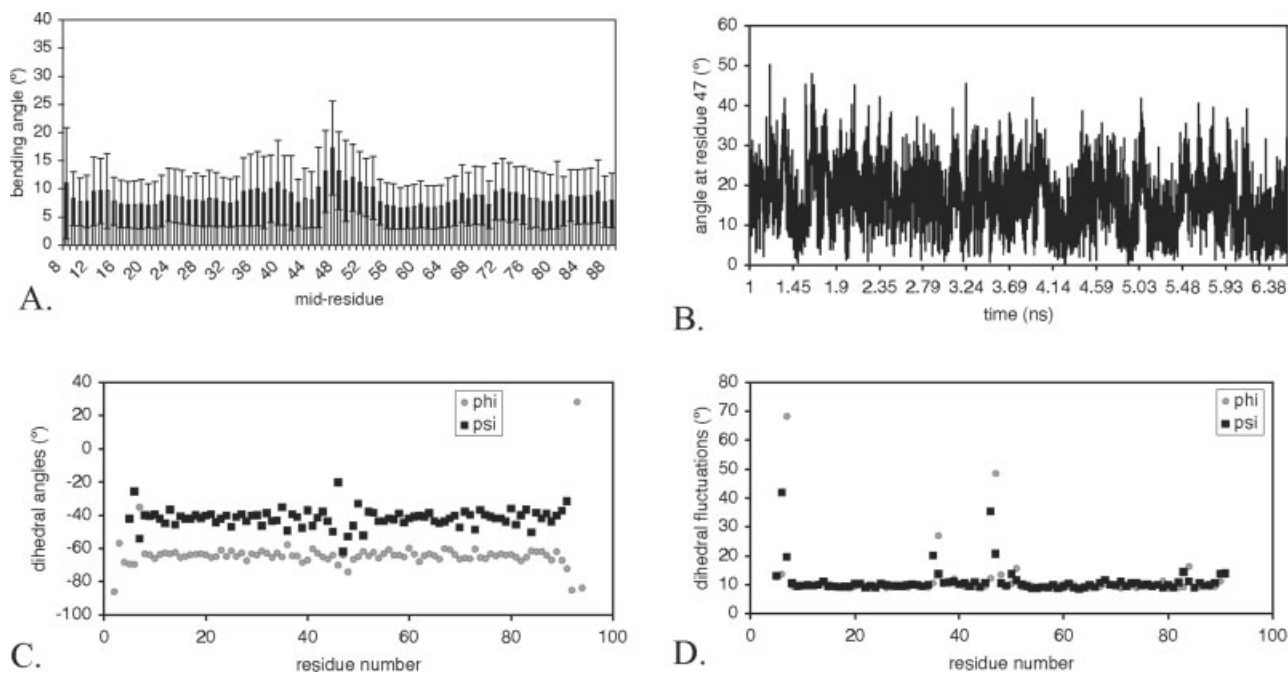


**Figure 4**

A: The average local bending angles; B: the bending angle at residue 47 as a function of time; C: average dihedral angles ( $\phi_i$  and  $\psi_i$ ); and D: their fluctuations during a MD simulation of the truncated  $\alpha$ -synuclein on a mixed membrane.

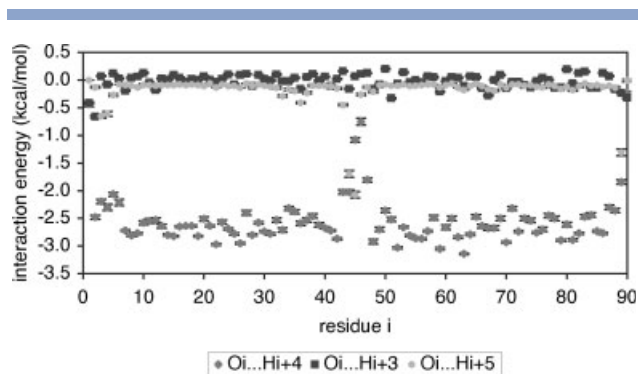


**Figure 5**

Interaction energy between  $O_i$  and  $H_{i+4}$  atoms,  $O_i$  and  $H_{i+3}$  atoms or  $O_i$  and  $H_{i+5}$  atoms, averaged between 1 and 6.57 ns of a MD simulation of the truncated  $\alpha$ -synuclein on a mixed membrane. Error bars are twice the standard deviation of the mean.

0.02 kcal/mol). The O of K45 is bonded to the H of V49 ( $-1.08 \pm 0.04$  kcal/mol) and to the H of H50 ( $-2.07 \pm 0.06$  kcal/mol), thus the  $i, i+5$  hydrogen bond is more frequent than the  $i, i+4$  hydrogen bond. The O of E46 only weakly interacts with the H of H50 ( $-0.75 \pm 0.06$  kcal/mol) and the H of G51 ( $-0.26 \pm 0.06$  kcal/mol). Similarly, the O of G47 is bonded to the H of G51 ( $-1.8 \pm 0.04$  kcal/mol) and to the H of V52 ( $-0.13 \pm 0.02$  kcal/mol). The usual  $O_i \dots H_{i+4}$  hydrogen bond network is resumed from V48 on.

The helix features a series of hydrogen bonds between the backbone and side-chain atoms. The backbone oxygen is often bonded to the HG1 of Thr (the average interaction energy is approximately  $-2.5$  kcal/mol), whereas the backbone hydrogen is bonded to the OG1 of Thr (the average interaction energy is approximately  $-1.2$  kcal/mol). Several threonines are located on the nonpolar face of the helix and are exposed to the membrane, in spite of their polarity (Fig. 6; Thr is colored in lime). These hydrogen bonds lower the penalty for having threonines in the apolar environment.

Lysine residues are important in binding; all twelve lysines are in the proximity of the membrane, with the NZ atom at  $\sim 17$ – $21$  Å (the position of the center of mass of lysines is shown in Fig. 6 as the dark blue diamond). The lysines are responsible for favorable protein–membrane electrostatic interactions. The side chains of some of the lysines partially embed into the headgroup region of the membrane, but not below the hydrophobic tail/headgroup interface as would correspond to snorkeling<sup>40</sup> in a classical sense. This is most frequent in K60, the CB and CG atoms of which are  $\sim 50\%$  of time at  $\sim 13.7 \pm 0.6$  Å; the CB, CG, CD, and CE atoms of lysines 12, 23, 45, 58, and 80 occasionally intercalate the membrane as well. The C-terminus of the  $\alpha$ -synuclein helix is

poor in lysines, implying that only weak protein–headgroup electrostatic interactions are feasible. A string of valines and threonines (in Fig. 6 shown as the pink and lime diamonds, respectively) however facilitates its binding to the membrane.

The truncated  $\alpha$ -synuclein contains two phenylalanines, F4 and F94, at its ends, which might anchor the protein on the membrane via hydrophobic interactions. Between 1 and 6.57 ns of a MD simulation, F4 is  $\sim 92\%$  of time embedded in the membrane, with the average position of the CZ atom at  $9.68 \pm 1.71$  Å, whereas the CZ atom of F94 is only  $\sim 21\%$  of time within the membrane (its average position is  $11.80 \pm 1.60$  Å). At longer times, F4 stays embedded in the membrane, while F94 gets exposed to solvent as the C-terminus moves away from the membrane. To test whether F94 would stay on the membrane within a somewhat longer helix, we performed a 12-ns MD simulation of the first 100 residues of  $\alpha$ -synuclein. The additional five residues are KKDQL, which might facilitate electrostatic interactions with charges on the membrane and/or hydrophobic interactions. However, as in the shorter helix, F94 moved away from the membrane. According to the measured effect of the aqueous spin label  $Mn^{2+}$  on backbone NMR resonances, F94 seems to be solvent-exposed in the micelle-bound  $\alpha$ -synuclein as well.<sup>46</sup>

All negatively charged amino acids are located exclusively in the polar face of the helix, with side chains extended towards solvent. Such an arrangement may reduce electrostatic repulsions between the negative charge of acidic residues and the membrane charges, as well as desolvation penalties, thus allowing the protein to approach the membrane closer than if the acidic residues

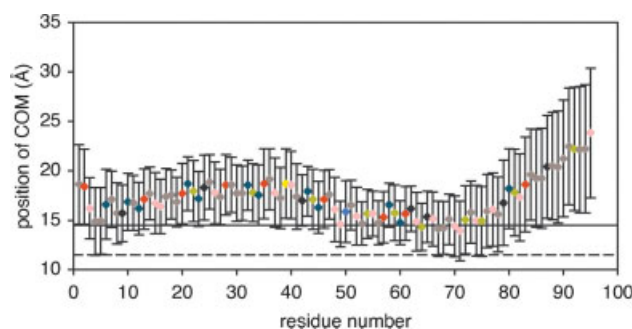


**Figure 6**

The average position of the center of mass (COM) of residues, between 1 and 6.57 ns of a MD simulation of the truncated  $\alpha$ -synuclein on a mixed membrane. Error bars are the standard deviation. The full line at 14.5 Å represents the position of the plane of smeared charges; the dashed line at 11.5 Å denotes the headgroup/hydrocarbon tail interface. The following color-coding of residues is used: Lys is dark blue, His is light blue, Glu or Asp is red, Tyr is yellow, Val is pink, Thr is lime, other hydrophobic residues are gray, and other hydrophilic residues are black.

were at the polar/nonpolar interface. For example, a study by Mishra *et al.* showed that a class A amphipathic helix interacts more strongly with anionic lipids than with zwitterionic lipids, whereas the opposite is true for a helix in which lysines are in the polar face and acidic residues are at the polar/nonpolar interface.<sup>67</sup> They attributed the lower affinity of the latter helix for anionic lipids to electrostatic repulsions between acidic residues and the lipid charges and to lower solvation of long hydrocarbon side chain of lysines than of shorter side chain of glutamates or aspartates. In the helical peptide VEEKS, derived from the membrane-binding domain of phosphocholine cytidyltransferase, three glutamates are located at the polar/nonpolar interface and binding to acidic membranes is pH-dependent.<sup>43,65</sup> The location of acidic residues in the polar face, not at the polar/nonpolar interface, may also discourage salt bridges that could interfere with lysine-membrane interactions.

As pointed out by Bussell *et al.* for  $\alpha$ -synuclein bound to micelles<sup>46</sup> and shown here in Figure 6 for the truncated  $\alpha$ -synuclein on the mixed membrane, a few residues around K12 interact strongly with the membrane, with their atoms near the headgroup/hydrocarbon tail interface. The region between residues 63–79 is most deeply buried, which is also in accordance with experimental studies.<sup>46,50</sup> The sole tyrosine of the truncated protein, Y39 (shown as the yellow diamond in Fig. 6), is located either at the membrane–solvent interface or is exposed to solvent, which is in agreement with Chandra *et al.*,<sup>24</sup> Bussell and Eliezer,<sup>25</sup> and Jao *et al.*,<sup>45</sup> but not with Bisaglia *et al.*<sup>50</sup> who predicted Y39 to be buried in the SDS micelle and suggested that the burial might protect  $\alpha$ -synuclein from aggregation as well as to protect Y39 from phosphorylation by p72<sup>syk</sup> tyrosine kinase.<sup>68</sup> The center of mass of the three residues, A30, A53, and E46, the mutation of which to proline, threonine, and lysine, respectively, is associated to PD,<sup>8–10</sup> is in the proximity of the membrane surface (the center of mass of A30, A53, and E46 is at  $17.74 \pm 2.86 \text{ \AA}$ ,  $14.67 \pm 2.17 \text{ \AA}$ , and  $17.10 \pm 2.92 \text{ \AA}$ ) and, thus, the mutation might influence binding to the membrane. The environmental exposure of residues in the optimal orientation determined here agrees well with that reported in an electron paramagnetic resonance study of  $\alpha$ -synuclein bound to SUVs containing 30 mol % of anionic lipids, at 0.1M salt, by Jao *et al.*<sup>45</sup> (see Fig. S2 in the supplementary material section).

### Helix bending

As shown in Figures 3 and 4, the helical truncated  $\alpha$ -synuclein bound to the mixed membrane is bent, most prominently near its middle (i.e., at residues 46–48). The bend location is close to the helix break on micelles, reported at residues 43–44,<sup>24</sup> 42–44,<sup>25</sup> and 38–44.<sup>26</sup> It has been suggested that the break is related to micelle

curvature<sup>24,25,45</sup> and that the break region can be more or less ordered depending on the micelles,<sup>26</sup> that the break facilitates contact between hydrophobic residues and membranes,<sup>24,25</sup> or that it is due to Y39.<sup>25</sup> We performed a series of tests to obtain insight into what causes the helix bend.

To test whether the bend is related to binding of the protein to the membrane, a MD simulation of the helical  $\alpha$ -synuclein was run in implicit water (EEF1.1)<sup>62,69</sup> and in implicit cyclohexane. Although  $\alpha$ -synuclein is a random coil in water,<sup>22</sup> we modeled it here as a helix in order to study helix bending as a function of environment. Bending of the helix in water [Fig. 7(A)] is comparable to that in the membrane-bound helix [Fig. 4(A)], being large at residues 45 ( $16.65^\circ \pm 16.91^\circ$ ) and 46 ( $16.54^\circ \pm 10.91^\circ$ ), but it is also significant at other locations, such as at residues 8, 51, and 72–75. The helix is bent in cyclohexane as well [Fig. 7(B,C)]. However, the bending angles are smaller and more delocalized than in water or on the membrane. On the basis of these data, we can rule out that bending of the helix is exclusively due to the membrane binding. Additional simulations showed that helix bending is not linked to protein sequence either; in fact, that bending was present in all long helices (see Fig. S3 and accompanying text in the supplementary material section). Thus, we conclude that bending is an intrinsic characteristic of long helices.

In Figure 3 it can be seen that  $\alpha$ -synuclein bound to the anionic membrane exhibits a wide range of bending motions during a MD simulation and, in Figure 4(B), that the bending angle at residue 47 oscillates between high values and values near zero (corresponding to the straight helix). Collective vibrations of the helix backbone in (Ala)<sub>20</sub> peptide, studied by MD, revealed that the bend vibrations are thrice slower than the stretch vibrations.<sup>70</sup> It follows from the elastic rod model<sup>71</sup> that, in a rod with free ends, the frequencies of the stretch ( $v^s$ ) and bend ( $v^b$ ) vibrations depend on the rod length ( $L$ ) and the elastic modulus ( $Y$ ) and are defined as

$$v^s = (1/2L)(Y/\rho)^{1/2} \quad (1)$$

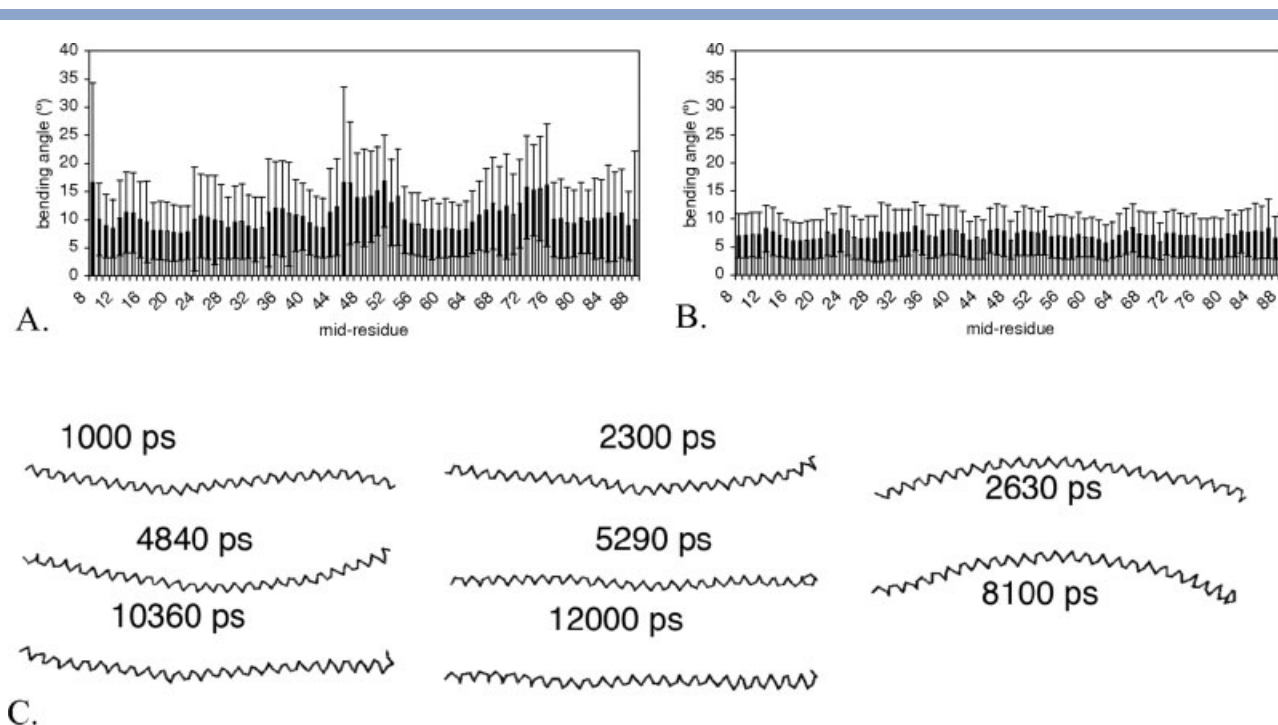
and

$$v^b = 1.12(R/L^2)(Y/\rho)^{1/2} \quad (2)$$

where  $R$  is the radius and  $\rho$  is the density. The ratio of the stretch and bend vibrations is thus

$$v^s/v^b = (1/2.24)(L/R). \quad (3)$$

Given the radius of the helix,  $R$ , of 0.45 nm and, for (Ala)<sub>20</sub> helix,  $L$  of 3 nm,  $v^s/v^b$  is 3; for the truncated

**Figure 7**

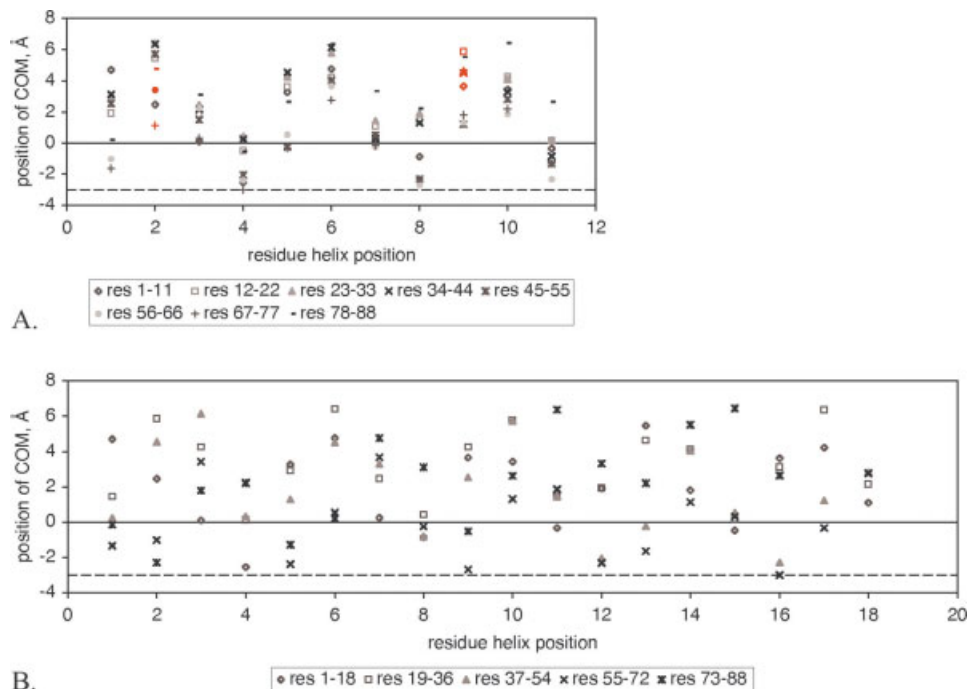
The average local bending angle of the  $\alpha$ -synuclein helix in water (A) and in cyclohexane (B); snapshots from a 12-ns MD of  $\alpha$ -synuclein in cyclohexane (C). The averages are calculated between 1 and 6 ns of MD simulations. The error bars are the standard deviation.

$\alpha$ -synuclein helix,  $L$  is 14.7 nm (assuming an ideal  $\alpha$ -helix), and thus  $v^s/v^b$  is 14.6. The bend vibrations are therefore  $\sim 15$  times slower than the stretch vibrations in  $\alpha$ -synuclein, giving rise to bending angles, as observed in our simulations.

### Helix periodicity

Several studies raised the question regarding the periodicity of the helix formed upon binding of  $\alpha$ -synuclein to membranes. Using site-directed spin-labeling, Jao *et al.* determined that repeats 5–7 of  $\alpha$ -synuclein bound to SUVs have 11/3 periodicity (i.e., 11 residues correspond to three full turns),<sup>45</sup> and later Bussell *et al.* confirmed that the SDS micelle-bound  $\alpha$ -synuclein exhibits the same periodicity,<sup>46</sup> as opposed to the 18/5 periodicity of an ideal  $\alpha$ -helix. To date, there are no data on the periodicity of  $\alpha$ -synuclein bound to LUVs. In 18/5 periodicity, there are 3.6 residues per turn and the rotation per residue is  $100^\circ$ . In 11/3 periodicity, the number of residues per turn is 3.67 and the rotation per residue is  $98.18^\circ$ . To determine the periodicity of the  $\alpha$ -synuclein helix in our simulations, we calculated the rotation per residue (aka twist angle,  $C_{\alpha,i} - C_{\alpha,i+3}$ ) and the number of residues per turn, using the HELANAL program,<sup>66</sup>

in the energy-minimized average conformation of the protein [shown in Fig. 3(B)] calculated from a MD trajectory between 1 and 6.57 ns (i.e., at the time period during which the protein binds to the mixed membrane lengthwise). The average twist angle for residues 2–93 is  $98.03 \pm 3.55^\circ$ ; the average number of residues per turn is  $3.68 \pm 0.16$ . These values imply that the helix periodicity is likely 11/3. To get a more conclusive proof, we plotted the position of the center of mass of each residue, relative to the membrane, against the position of the residue in a 11-residue repeat [Fig. 8(A)] and in a 18-residue repeat [Fig. 8(B)]. That is, the sequence from residues 1 to 88 is divided into windows, each 11 or 18 amino acids long, and the windows are superimposed so that the residue  $i$  is at the same position as the residue  $i + 11$ , or, in the case of the  $\alpha$ 18/5 helix, the residue  $i + 18$ . If there is a clear trend in the positions of the center of mass of each residue in the superimposed windows that repeats after the given number of turns, the periodicity is satisfied. The points cluster much better in Figure 8(A) than in Figure 8(B), which clearly demonstrates that, in  $\alpha$ -synuclein bound to the mixed membrane, the helix periodicity is much closer to 11/3. The same trend is observed in the position of the  $C_\alpha$  atom of each residue (data not shown).

**Figure 8**

The position of the center of mass of each residue (COM) in the energy-minimized average conformation of  $\alpha$ -synuclein on a mixed membrane, relative to the plane of smeared charges (PSC), (A) for 11/3 periodicity or (B) for 18/5 periodicity. The full line represents the position of PSC, which is taken as the reference point and corresponds to 14.5 Å; the dashed line represents the position of the headgroup/hydrocarbon tail interface. The average conformation is calculated from a MD trajectory between 1 and 6.57 ns. In (A) the first residues of the seven repeats are colored in red.

Figure 8(A) further says that the residues at positions 4, 8, and 11 are closer to the membrane than those at other positions, whereas the residues at positions 2, 6, and 9 are exposed to solvent; residues at position 1, 3, 5, 7, and 10 are at the interface. Such an arrangement is tantamount to the 11/3 helical pinwheel.<sup>25</sup> Lysines are mostly found at positions 1, 3, and 10, whereas glutamates and an aspartate are at positions 2 and 6; a number of threonines, characteristic for  $\alpha$ -synuclein, are in the non-polar face of the helix (i.e., at positions 4 and 11). Regarding the seven 11-residue repeats, the first residue of repeats 1–4 is at position 9, whereas the first residue of repeats 5–7 is shifted to position 2 due to the four residues (ATVA) that demarcate repeats 4 and 5. However, this shift does not break the periodicity since both positions are equivalent with respect to the membrane proximity and the environmental exposure (that is, both are in the polar face of the helix and solvent-exposed). We conclude that the periodicity of  $\alpha$ -synuclein is indeed 11/3, and that, through positioning of charged residues, it has implications on membrane binding.

### Energetics of the 11/3 and 18/5 helices

To get some insight into why the  $\alpha$ -synuclein helix bound to the anionic membrane prefers 11/3 instead of

18/5 periodicity, we performed 1-ns MD simulations in water or on the anionic membrane, starting from the ideal 18/5 or 11/3 helix. To preserve the periodicity, the dihedral angles were constrained to their ideal values ( $\phi_i = -57^\circ$ ,  $\psi_i = -47^\circ$  in the 18/5 helix;  $\phi_i = -58.7^\circ$ ,  $\psi_i = -48.8^\circ$  in the 11/3 helix)<sup>44</sup> before energy minimization and molecular dynamics. Since the 18/5 helix does not bind to the membrane as tightly as the 11/3 helix, the center of mass of the helices was prevented from exiting a cylinder of 17 Å radius (with the axis of the cylinder along the  $x$ -axis), using the miscellaneous mean-field potential (MMFP) facility of CHARMM. This led to comparable average position of the center of mass of the helices during the simulations ( $16.15 \pm 0.40$  Å and  $16.88 \pm 0.22$  Å for the 11/3 and the 18/5 helix, respectively). The average energies were calculated from the last 800 ps of the simulations.

In water, the transition from the 18/5 to 11/3 helix involves a change in the average effective energy,  $\langle \Delta W \rangle$ , of  $12.35 \pm 1.13$  kcal/mol, mostly due to the van der Waals ( $\langle \Delta W_{\text{vdw}} \rangle = 12.56 \pm 0.89$  kcal/mol) and electrostatic ( $\langle \Delta W_{\text{elec}} \rangle = 14.44 \pm 0.96$  kcal/mol) energies; the solvation energy components due to polar, aliphatic and aromatic groups are  $\langle \Delta W_{\text{polar}} \rangle = -12.62 \pm 0.45$  kcal/mol,  $\langle \Delta W_{\text{alip}} \rangle = 0.47 \pm 0.03$  kcal/mol, and  $\langle \Delta W_{\text{arom}} \rangle = 0.01 \pm 0.01$  kcal/mol, respectively. However,  $\langle \Delta W \rangle$

for the same transition on the anionic membrane is  $-4.93 \pm 1.09$  kcal/mol ( $\langle \Delta W_{\text{vdw}} \rangle = 13.66 \pm 0.85$  kcal/mol,  $\langle \Delta W_{\text{elec}} \rangle = -2.29 \pm 0.95$  kcal/mol,  $\langle \Delta W_{\text{polar}} \rangle = -7.85 \pm 0.66$  kcal/mol,  $\langle \Delta W_{\text{alip}} \rangle = -3.65 \pm 0.27$  kcal/mol, and  $\langle \Delta W_{\text{arom}} \rangle = -1.37 \pm 0.03$  kcal/mol). Therefore, because of more favorable solvation of polar groups and hydrophobic interactions, the membrane-bound 11/3 helix is energetically more stable than the 18/5 helix. Compared to the energy of the helix in water, the effective energy of the 11/3 helix is by  $23.80 \pm 1.10$  kcal/mol lower on the membrane ( $\langle \Delta W_{\text{vdw}} \rangle = -3.97 \pm 0.87$  kcal/mol,  $\langle \Delta W_{\text{elec}} \rangle = -22.29 \pm 0.95$  kcal/mol,  $\langle \Delta W_{\text{polar}} \rangle = 39.36 \pm 0.56$  kcal/mol,  $\langle \Delta W_{\text{alip}} \rangle = -30.74 \pm 0.23$  kcal/mol, and  $\langle \Delta W_{\text{arom}} \rangle = -1.58 \pm 0.02$  kcal/mol); the effective energy of the membrane-bound 18/5 helix is  $6.52 \pm 1.11$  kcal/mol lower than the helix in water ( $\langle \Delta W_{\text{vdw}} \rangle = 2.87 \pm 0.88$  kcal/mol,  $\langle \Delta W_{\text{elec}} \rangle = -5.56 \pm 0.96$  kcal/mol,  $\langle \Delta W_{\text{polar}} \rangle = 34.59 \pm 0.56$  kcal/mol,  $\langle \Delta W_{\text{alip}} \rangle = -26.61 \pm 0.15$  kcal/mol, and  $\langle \Delta W_{\text{arom}} \rangle = -0.19 \pm 0.02$  kcal/mol). The electrostatic interactions with the negative charge on the membrane are similar regardless of the helix periodicity (the GC term is  $-10.46 \pm 0.04$  kcal/mol for the 11/3 helix and  $-9.12 \pm 0.05$  kcal/mol for the 18/5 helix), but 11/3 periodicity allows more favorable solvation effects ( $-15.24$  kcal/mol in the 11/3 helix vs.  $2.22$  kcal/mol in the 18/5 helix, calculated as  $\langle \Delta W_{\text{elec}} \rangle + \langle W_{\text{polar}} \rangle + \langle W_{\text{alip}} \rangle + \langle W_{\text{arom}} \rangle$ ). This observation is in agreement with predictions of Segrest and coworkers that 11/3 periodicity aligns hydrophobic residues to form a continuous nonpolar face of the helix and increases lipid affinity, which can offset the cost of 18/5 to 11/3 helix transition.<sup>44,72</sup>

### $\alpha$ -Synuclein dimer on a mixed membrane

The lack of consensus on the role of membranes and/or of the helical conformation in aggregation and fibrillation motivated us to perform simulations of an  $\alpha$ -synuclein dimer on the mixed membrane in order to determine whether dimerization is energetically feasible and how it affects membrane binding.

On the basis of the effective energies, averaged over the last 11 ns of 12-ns MD simulations, performed using four different random numbers, the antiparallel dimer is  $\sim 28$  kcal/mol more favorable than the parallel dimer (Table I). Relative to the effective energy of two noninteracting monomers, dimerization is energetically favorable. The average interaction energy between two monomers in the antiparallel dimer is  $-73.50 \pm 0.26$  kcal/mol ( $\langle W_{\text{vdw}} \rangle = -131.35 \pm 0.37$  kcal/mol;  $\langle W_{\text{elec}} \rangle = -26.87 \pm 0.24$  kcal/mol and  $\langle W_{\text{solv}} \rangle = 84.73 \pm 0.31$  kcal/mol); that in the parallel dimer is  $-55.34 \pm 0.30$  kcal/mol ( $\langle W_{\text{vdw}} \rangle = -98.67 \pm 0.40$  kcal/mol;  $\langle W_{\text{elec}} \rangle = -20.33 \pm 0.20$  kcal/mol and  $\langle W_{\text{solv}} \rangle = 63.66 \pm 0.29$  kcal/mol). Thus, dimerization is mainly driven by the van der Waals energy.

The average transfer effective energies of the antiparallel and parallel dimers are  $\sim 2$ – $3$  kcal/mol more positive than that of two noninteracting monomers (Table I). The main difference in effective energies of the dimers versus monomers comes from the Gouy-Chapman energy term; it is more favorable for monomers than for the parallel dimer and even more so than for the antiparallel dimer, suggesting that some lysines that facilitate interactions of monomeric  $\alpha$ -synuclein with the headgroups are instead involved in protein–protein interactions.

Figure 9(A) shows snapshots from a 12-ns MD simulation of the antiparallel dimer on the mixed membrane. Compared to monomeric  $\alpha$ -synuclein under the same conditions [Fig. 3(A)], the dimer is more displaced from the membrane surface, with only a few residues embedded in the headgroup region. Some lysines are at the protein–membrane interface but many are exposed to solvent or are at the protein–protein interface. Hydrophobic residues within the C-terminal half of one monomer, including residues 71–82 found to promote fibrillation and aggregation of wild type  $\alpha$ -synuclein in solution,<sup>47</sup> rarely interact with the membrane but engage in interactions with the N-terminal half of the second monomer. Even when they intercalate in the membrane, as, for instance, at 3.16 ns, dimerization is not suppressed.

As in the monomer, bending motions are present in the dimer. The location of the largest bending angles is shifted from the middle of monomer to residues 53–57 in the chain more displaced from the membrane (chain 1) and to residues 18–20 in the other chain. Both helices in the antiparallel dimer experience destabilization relative to monomer, which is more pronounced in the helix closer to the membrane (chain 2). The average interaction energy between the backbone  $O_i$  and  $H_{i+4}$  atoms is less favorable in chain 2 than in chain 1 or in monomer (Fig. 5), whereas the average interaction energy between the backbone  $O_i$  and  $H_{i+5}$  atoms is more favorable. Dihedral angles ( $\phi_i$  and  $\psi_i$ ) and their fluctuations are also more perturbed in chain 2 than in chain 1 or in monomer [Fig. 4(C,D)].

The calculated average twist angle (the average number of residues per turn) is  $98.52^\circ \pm 2.38^\circ$  ( $3.66 \pm 0.09$ ) for residues 2–93 of chain 1 in the energy-minimized average conformation, calculated over the last 11 ns of a 12-ns MD simulation, whereas that for the same residues of chain 2 is  $96.68^\circ \pm 5.38^\circ$  ( $3.74 \pm 0.24$ ). Although the effect of dimerization on helix periodicity is not apparent from the calculated twist angles due to the large error bars, the plot of the position of the center of mass of residues versus the residue helix position (Fig. 10) reveals some discrepancies compared with the same plots for monomer (Fig. 8). According to the 18/5 plot (the lower plot of Fig. 10(A)), the periodicity of the helix more displaced from the membrane is closer to 18/5 than to 11/3. The periodicity of the other helix seems to be 11/3 [Fig. 10(B)], though the position of the center of mass of

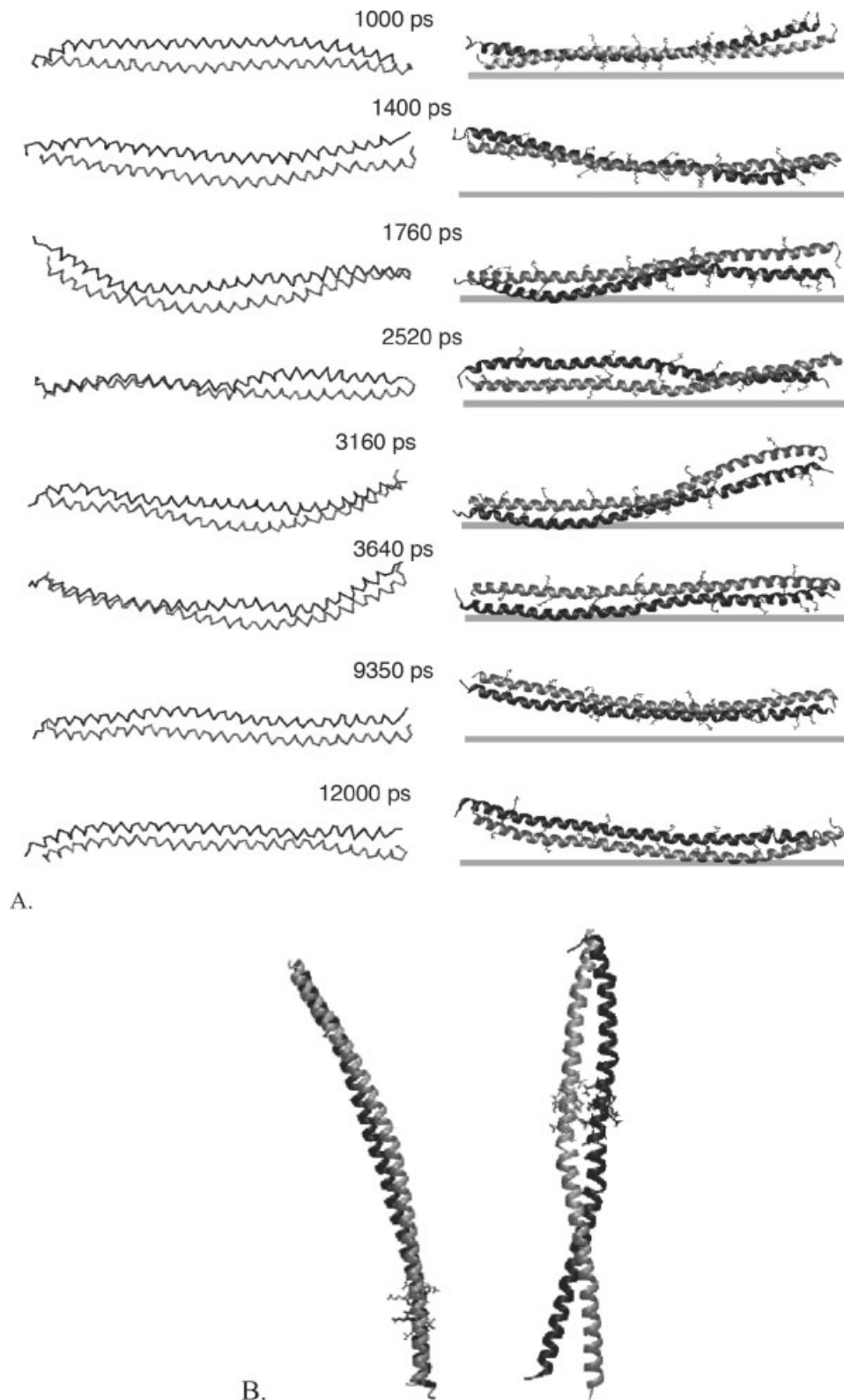


### Figure 9

*A: Snapshots of a  $\alpha$ -synuclein antiparallel dimer on a mixed membrane taken from a 12-ns MD simulation. See the caption of Figure 3 for the membrane description. The residues shown in stick representation are lysines. B: Coiled coils formed by the energy-minimized average structure of the antiparallel (on the left) and parallel (on the right) dimers. The structure was averaged over the last 11 ns of simulations on the mixed membrane. The residues with the knobs-into-holes side chain packing are shown as sticks; chain 1 is shown in gray; chain 2 is shown in black.*

residues 1–16, relative to the membrane, is somewhat shifted when compared with the other residues. These data imply that, in order to accommodate protein–protein interactions, the helices undergo subtle conformational changes.

Because of the 11/3 periodicity of monomeric  $\alpha$ -synuclein, it has been suggested that  $\alpha$ -synuclein might form a rare right-handed coiled coil,<sup>25</sup> characterized by an undecad repeat in lieu of a heptad repeat of a left-handed coiled coil.<sup>73</sup> To check whether  $\alpha$ -synuclein

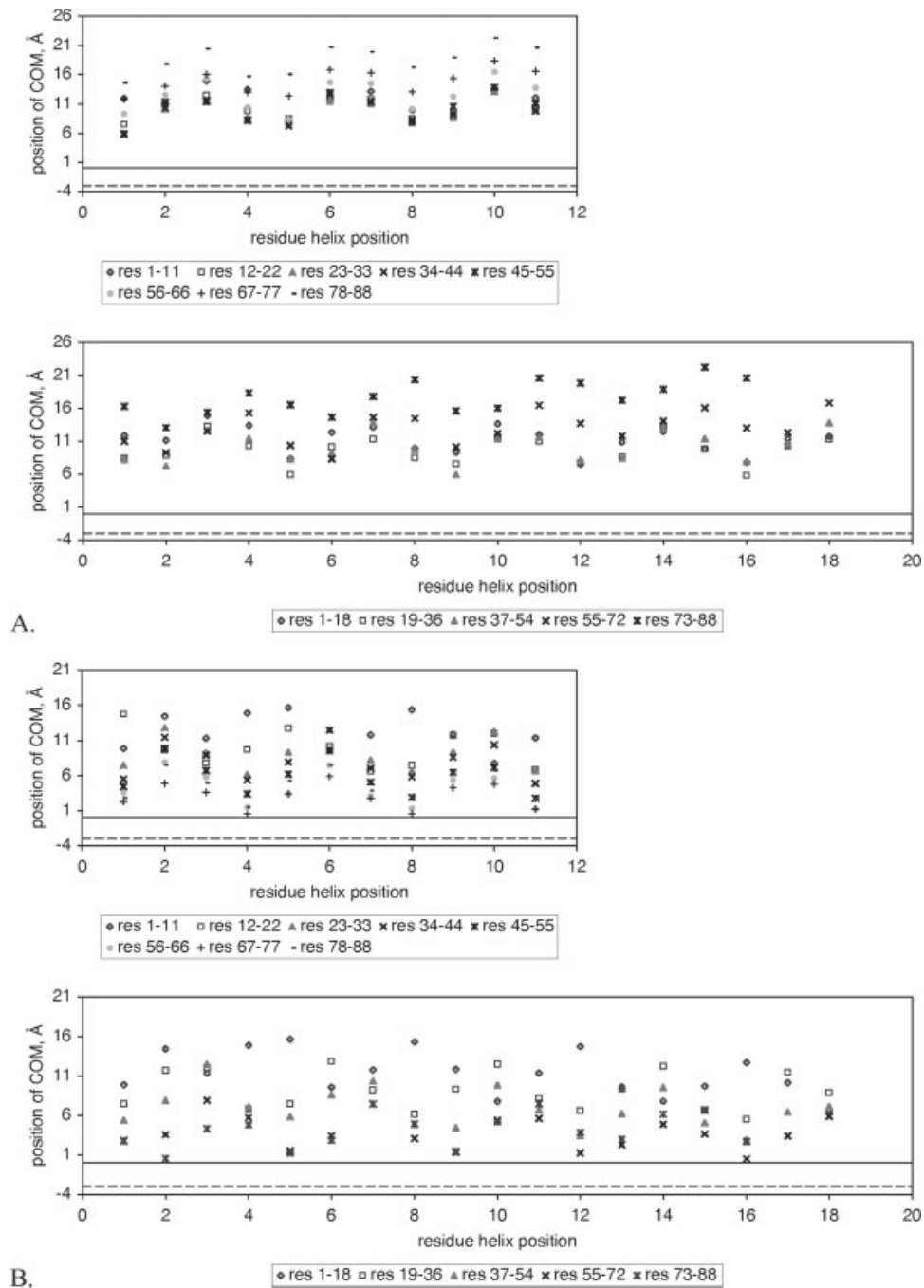


**Figure 10**

The position of the center of mass of each residue (COM) of (A) chain 1 and (B) chain 2 of an antiparallel dimer on the mixed membrane, relative to the plane of smeared charges (PSC), for 11/3 periodicity (the upper plot) or for 18/5 periodicity (the lower plot). The solid line represents the position of PSC, which is taken as the reference point and corresponds to 14.5 Å; the dashed line represents the position of the headgroup/hydrocarbon tail interface.

dimers form coiled coil structures, we used the SOCKET program<sup>74</sup> to search for the required knobs-into-holes side chain packing in the energy-minimized average structure of the antiparallel and parallel dimer. A coiled coil was identified in both dimers. In the antiparallel dimer [shown on the left in Fig. 9(B)], the knobs-into-holes packing extends over 11 residues: residues 13–23 (EGVVAAAEKTK) of chain 1 and residues 72–82 (TGVTAQAQKTV) of chain 2, resulting in a right-handed coiled-coil. In the parallel dimer [shown on the right in Fig. 9(B)], the packing is again 11-residue long and involves residues 54–64 (TVAEKTKEQVT) of chain 1 and residues 52–62 (VATVAEKTKEQ) of chain 2, but the coiled coil is left-handed.

Taken together, these results suggest that at low surface concentration of  $\alpha$ -synuclein, at which protein–protein interactions are prevented, the C-terminal hydrophobic residues embed in the membrane, whereas at high surface concentration, the same residues promote protein–protein interactions, at a slight expense of membrane–protein interactions.

## DISCUSSION

We report here a computational study of the binding of truncated  $\alpha$ -synuclein (residues 1–95) to planar bilayers. The key findings of the study are as follows: (1) the protein conformation on a mixed membrane is a bent helix, oriented in such a way that hydrophobic residues and a series of threonines are exposed to the membrane, lysines are at the hydrophilic/hydrophobic interface, and glutamates are exposed to solvent; (2) the helix bend is not related to membrane–protein interactions and is not sequence dependent; (3) the helix periodicity is 11/3 (that is, 11 residues makes up three full turns); (4) the truncated  $\alpha$ -synuclein prefers anionic membranes but also binds to a neutral membrane; (5) both protein–headgroup electrostatic interactions and hydrophobic interactions are responsible for binding to the mixed membrane; and (6) dimerization of  $\alpha$ -synuclein bound to the mixed membrane is energetically favorable.

The implicit membrane model used here is a convenient tool for studying protein–membrane interactions. However, one needs to keep in mind a number of limitations. In IMM1, the membrane is modeled as a hydrophobic slab and thus neglects, for example, membrane deformations, the membrane curvature, lipid reorganization induced by the presence of proteins, or specific interactions between amino acids and the headgroups. Furthermore, the Gouy-Chapman theory neglects discrete charge effects and cannot account for local charge fluctuations as present in lipid demixing. Theoretical studies showed that charged macromolecules bind more strongly to membranes when lipids can undergo lateral diffusion and reorganize in the vicinity of the binding site.<sup>75,76</sup>

Given that experimental studies reported that  $\alpha$ -synuclein may induce the lateral segregation of the lipids in a mixed membrane<sup>77</sup> and that its binding affinity depends on the chemical nature of the lipids and/or lipid packing,<sup>22,27–31</sup> the binding energies and penetration depth of the helix reported here might be somewhat underestimated.

As a peripheral protein,  $\alpha$ -synuclein does not penetrate deep in the membrane core.<sup>30,46</sup> Jao *et al.* estimated that the center of the  $\alpha$ -synuclein helix bound to SUVs is located at an immersion depth of  $\sim 1$ – $4$  Å below the phosphates.<sup>45</sup> In our simulations, during the time period at which both termini of the protein are bound to the mixed membrane, the center of mass of the helix is at  $\sim 17$  Å, or, around  $2.5$  Å above the phosphates. The position of the most buried  $C_{\alpha}$  atoms is at  $12$ – $14$  Å, or  $2.5$ – $0.5$  Å below the phosphates. A slight discrepancy in the location of the center of the helix could be due to differences in the curvature of vesicles used in experiment and simulation. Proteins often bind more strongly to SUVs than to LUVs, as a consequence of differences in lipid packing induced by the curvature.<sup>78–81</sup>

The  $\alpha$ -synuclein helix bound to the mixed membrane is bent, with the largest bend about residue 47. Other groups have also observed bending in the middle of a helix during simulations.<sup>82–84</sup> Recently, Zagrovic *et al.* measured the radius of gyration of alanine-based peptides of different length. They found that, as the length of the peptide increases, the radius of gyration becomes smaller than that of an ideal  $\alpha$ -helix, and suggested that the longer helices have to be bent somewhere in the middle.<sup>85</sup> We showed herein that bending of the  $\alpha$ -synuclein helix is related to delocalized bending vibrations. It is noteworthy that, as the helix length increases, bending vibrations lag the stretching vibrations more, implying that short helices tend to stretch whereas long helices tend to bend.

Lee *et al.* hypothesized that formation of amyloid fibrils of  $\alpha$ -synuclein involves transition from  $\alpha$ -helix to  $\beta$ -sheet via partially folded intermediates.<sup>56</sup> Such a pathway has been recognized in other proteins such as human islet amyloid polypeptide,<sup>86</sup> amyloid  $\beta$ -protein,<sup>87</sup> insulin,<sup>88</sup> and a helix-turn-helix model peptide.<sup>89</sup> Our finding that dimerization of  $\alpha$ -synuclein is energetically favorable suggests that an initial step in fibrillation might be oligomerization of membrane-bound helical monomers, accompanied by destabilization of the helical structure, which could further lead to formation of a predominantly  $\beta$ -sheet conformation. Interestingly, as has been reported recently,  $\alpha$ -synuclein fibrils become unstable in the presence of a large concentration of SDS micelles, accompanied by  $\beta$ -sheet to  $\alpha$ -helix transition.<sup>59</sup> Zhu *et al.* found that a negatively charged mica surface significantly speeds up the growth of fibrils of amyloidogenic light chain variable domain at low protein concentration and under conditions at which the fibrillation does not

occur in solution.<sup>90</sup> They postulated that association of the protein with a surface could increase the local concentration of the protein, resulting in faster fibril formation. The weaker membrane–dimer interactions that we observed could facilitate lateral diffusion of the protein on the membrane surface, leading to formation of higher-molecular-weight oligomers and, ultimately, fibrils.

## ACKNOWLEDGMENT

We are grateful to Dr. David Eliezer for invaluable discussions and comments on the manuscript.

## REFERENCES

- Maroteaux L, Scheller RH. The rat brain synucleins; family of proteins transiently associated with neuronal membrane. *Brain Res Mol Brain Res* 1991;11:335–343.
- Lavedan C. The synuclein family. *Genome Res* 1998;8:871–880.
- Spillantini MG, Schmidt ML, Lee VM-Y, Trojanowski JQ, Jakes R, Goedert M.  $\alpha$ -Synuclein in Lewy bodies. *Nature* 1997;388:839–840.
- Spillantini MG, Crowther RA, Jakes R, Hasegawa M, Goedert M.  $\alpha$ -Synuclein in filamentous inclusions of Lewy bodies from Parkinson's disease and dementia with Lewy bodies. *Proc Natl Acad Sci USA* 1998;95:6469–6473.
- Uéda K, Fukushima H, Masliah E, Xia Y, Iwai A, Yoshimoto M, Otero DAC, Kondo J, Ihara Y, Saitoh T. Molecular cloning of cDNA encoding an unrecognized component of amyloid in Alzheimer disease. *Proc Natl Acad Sci USA* 1993;90:11282–11286.
- Lippa CF, Schmidt ML, Lee VM-Y, Trojanowski JQ. Antibodies to  $\alpha$ -synuclein detect lewy bodies in many Down's syndrome brains with Alzheimer's disease. *Ann Neurol* 1999;45:353–357.
- Galvin JE, Giasson B, Hurtig HI, Lee VM-Y, Trojanowski JQ. Neurodegeneration with brain iron accumulation, type 1 is characterized by  $\alpha$ -,  $\beta$ -, and  $\gamma$ -synuclein neuropathology. *Am J Pathol* 2000;157:361–368.
- Krüger R, Kuhn W, Müller T, Woitalla D, Graeber M, Kössel S, Przuntek H, Eppelen JT, L. S., Riess O. Ala30Pro mutation in the gene encoding  $\alpha$ -synuclein in Parkinson's disease. *Nat Genet* 1998;18:106–108.
- Zarranz JJ, Alegre J, Gómez-Esteban JC, Lezcano E, Ros R, Ampuero I, Vidal L, Hoenicka J, Rodriguez O, Atarés B, Llorens V, Tortosa EG, del Ser T, Muñoz DG, de Yébenes JG. The new mutation. E46K, of  $\alpha$ -synuclein causes Parkinson and Lewy body dementia. *Ann Neurol* 2004;55:164–173.
- Polymeropoulos MH, Lavedan C, Leroy E, Ide SE, Dehijia A, Dutra A, Pike B, Root H, Rubenstein J, Boyer R, Stenroos S, Chandrasekharappa S, Athanassiadou A, Papapetropoulos T, Johnson WG, Lazzarini AM, Duvoisin RC, Di Iorio G, Golbe LI, Nussbaum RL. Mutation in the  $\alpha$ -synuclein gene identified in families with Parkinson's disease. *Science* 1997;276:2045–2047.
- Sharon R, Goldberg MS, Bar-Josef MS, Betensky RA, Shen J, Selkoe DJ.  $\alpha$ -Synuclein occurs in lipid-rich high molecular weight complexes, binds fatty acids, and shows homology to the fatty acid-binding proteins. *Proc Natl Acad Sci USA* 2001;98:9110–9115.
- Golovko MY, Faergeman NJ, Cole NB, Castagnet PI, Nussbaum RL, Murphy EJ.  $\alpha$ -Synuclein gene deletion decreases brain palmitate uptake and alters the palmitate metabolism in the absence of  $\alpha$ -synuclein palmitate binding. *Biochemistry* 2005;44:8251–8259.
- George JM, Jin H, Woods WS, Clayton DF. Characterization of a novel protein regulated during the critical period for song learning in the zebra finch. *Neuron* 1995;15:361–372.
- Jenco JM, Rawlingson A, Daniels B, Morris AJ. Regulation of phospholipase D2: selective inhibition of mammalian phospholipase D isoenzymes by  $\alpha$ - and  $\beta$ -synucleins. *Biochemistry* 1998;37:4901–4909.
- Payton JE, Perrin RJ, Woods WS, George JM. Structural determinants of PLD2 inhibition by  $\alpha$ -synuclein. *J Mol Biol* 2004;337:1001–1009.
- Murphy DD, Rueter SM, Trojanowski JQ, Lee VM-Y. Synucleins are developmentally expressed, and  $\alpha$ -synuclein regulates the size of the presynaptic vesicular pool in primary hippocampal neurons. *J Neurosci* 2000;20:3214–3220.
- Cabin DE, Shimazu K, Murphy D, Cole NB, Gottschalk W, McIlwain KL, Orrison B, Chen A, Ellis CE, Paylor R, Lu B, Nussbaum RL. Synaptic vesicle depletion correlates with attenuated synaptic responses to prolonged repetitive stimulation in mice lacking  $\alpha$ -synuclein. *J Neurosci* 2002;22:8797–8807.
- Abeliovich A, Schmitz Y, Fariñas I, Choi-Lundberg D, Ho W-H, Castillo PE, Shinsky N, Verdugo JMG, Armanini M, Ryan A, Hynes M, Phillips H, Sulzer D, Rosenthal A. Mice lacking  $\alpha$ -synuclein display functional deficits in the nigrostriatal dopamine system. *Neuron* 2000;25:239–252.
- Chandra S, Fornai F, Kwon H-B, Yazdani U, Atasoy D, Liu X, Hammer RE, Battaglia G, German DC, Castillo PE, Südhof TC. Double-knockout mice for  $\alpha$ - and  $\beta$ -synucleins: effect on synaptic functions. *Proc Natl Acad Sci USA* 2004;101:14966–14971.
- Yavich L, Tanila H, Vepsäläinen S, Jäkälä P. Role of  $\alpha$ -synuclein in presynaptic dopamine recruitment. *J Neurosci* 2004;24:11165–11170.
- Chandra S, Gallardo G, Fernández-Chacón R, Schlüter OM, Südhof TC.  $\alpha$ -Synuclein cooperates with CSP in preventing neurodegeneration. *Cell* 2005;123:383–396.
- Davidson WS, Jonas A, Clayton DF, George JM. Stabilization of  $\alpha$ -synuclein secondary structure upon binding to synthetic membranes. *J Biol Chem* 1998;273:9443–9449.
- Eliezer D, Kutluay E, Bussell R, Jr, Browne G. Conformational properties of  $\alpha$ -synuclein in its free and lipid-associated states. *J Mol Biol* 2001;307:1061–1073.
- Chandra S, Chen X, Rizo J, Jahn R, Südhof TC. A broken  $\alpha$ -helix in folded  $\alpha$ -synuclein. *J Biol Chem* 2003;278:15313–15318.
- Bussell R, Jr, Eliezer D. A structural and functional role for 11-mer repeats in  $\alpha$ -synuclein and other exchangeable lipid binding proteins. *J Mol Biol* 2003;329:763–778.
- Ulmer TS, Bax A, Cole NB, Nussbaum RL. Structure and dynamics of micelle-bound human  $\alpha$ -synuclein. *J Biol Chem* 2005;280:9595–9603.
- Zhu M, Li J, Fink AL. The association of  $\alpha$ -synuclein with membranes affects bilayer structure, stability, and fibril formation. *J Biol Chem* 2003;278:40186–40197.
- Jo E, McLaurin J, Yip CM, St George-Hyslop P, Fraser PE.  $\alpha$ -Synuclein membrane interactions and lipid specificity. *J Biol Chem* 2000;275:34328–34334.
- Zhu M, Fink AL. Lipid binding inhibits  $\alpha$ -synuclein fibril formation. *J Biol Chem* 2003;278:16873–16877.
- Ramakrishnan M, Jensen PH, Marsh D.  $\alpha$ -Synuclein association with phosphatidylglycerol probed by lipid spin labels. *Biochemistry* 2003;42:12919–12926.
- Nuscher B, Kamp F, Mehnert T, Odoy S, Haass C, Kahle PJ, Beyer K.  $\alpha$ -Synuclein has a high affinity for packing defects in a bilayer membrane. *J Biol Chem* 2004;279:21966–21975.
- Narayanan V, Scarlata S. Membrane binding and self-association of  $\alpha$ -synucleins. *Biochemistry* 2001;40:9927–9934.
- Ramakrishnan M, Jensen PH, Marsh D. Association of  $\alpha$ -synuclein and mutants with lipid membranes: spin-label ESR and polarized IR. *Biochemistry* 2006;45:3386–3395.
- Kamp F, Beyer K. Binding of  $\alpha$ -synuclein affects the lipid packing in bilayers of small vesicles. *J Biol Chem* 2006;281:9251–9259.
- Rhoades E, Ramlall TF, Webb WW, Eliezer D. Quantification of  $\alpha$ -synuclein binding to lipid vesicles using fluorescence correlation spectroscopy. *Biophys J* 2006;90:4692–4700.
- Wood SJ, Wypych J, Steavenson S, Loius J-C, Citron M, Biere AL.  $\alpha$ -Synuclein fibrillogenesis is nucleation-dependent. *J Biol Chem* 1999;274:19509–19512.

37. Conway KA, Lee S-J, Rochet J-C, Ding TT, Williamson RE, Lansbury PT, Jr. Acceleration of oligomerization, not fibrillization, is a shared property of both  $\alpha$ -synuclein mutations linked to early-onset Parkinson's disease: implications for pathogenesis and therapy. *Proc Natl Acad Sci USA* 2000;97:571–576.
38. Volles MJ, Lansbury PT, Jr. Zeroing in on the pathogenic form of  $\alpha$ -synuclein and its mechanism of neurotoxicity in Parkinson's disease. *Biochemistry* 2003;42:7871–7878.
39. Shults CW. Lewy bodies. *Proc Natl Acad Sci USA* 2006;103:1661–1668.
40. Segrest JP, De Loof H, Dohlman JG, Brouillette CG, Anantharamaiah GM. Amphipathic helix motif: classes and properties. *Proteins: Struct Funct Genet* 1990;8:103–117.
41. Segrest JP, Jones MK, De Loof H, Brouillette CG, Venkatachalapathi YV, Anantharamaiah GM. The amphipathic helix in the exchangeable apolipoproteins: a review of secondary structure and function. *J Lipid Res* 1992;33:141–166.
42. Dunne SJ, Cornell RB, Johnson JE, Glover NR, Tracey AS. Structure of the membrane binding domain of CTP: phosphocholine cytidyltransferase. *Biochemistry* 1996;35:11975–11984.
43. Johnson JE, Xie M, Singh LMR, Edge R, Cornell RB. Both acidic and basic amino acids in an amphitropic enzyme. CTP: phosphocholine cytidyltransferase, dictate its selectivity for anionic membranes. *J Biol Chem* 2003;278:514–522.
44. Segrest JP, Jones MK, Klon AE, Sheldahl CJ, Hellinger M, De Loof H, Harvey SC. A Detailed molecular belt model for apolipoprotein A-I in discoidal high density lipoprotein. *J Biol Chem* 1999;274:31755–31758.
45. Jao CC, Der-Sarkissian A, Chen J, Langen R. Structure of membrane-bound  $\alpha$ -synuclein studied by site-directed spin labeling. *Proc Natl Acad Sci USA* 2004;101:8331–8336.
46. Bussell R, Jr, Ramallal TF, Eliezer D. Helix periodicity, topology, and dynamics of membrane-associated  $\alpha$ -synuclein. *Protein Sci* 2005;14:862–872.
47. Giasson BI, Murray IVJ, Trojanowski JQ, Lee VM-Y. A hydrophobic stretch of 12 amino acid residues in the middle of  $\alpha$ -synuclein is essential for filament assembly. *J Biol Chem* 2001;276:2380–2386.
48. Uversky VN, Li J, Souillac P, Millett IS, Doniach S, Jakes R, Goedert M, Fink AL. Biophysical properties of the synucleins and their propensities to fibrillate. *J Biol Chem* 2002;277:11970–11978.
49. Park J-Y, Lansbury PT, Jr.  $\beta$ -Synuclein inhibits formation of  $\alpha$ -synuclein protofibrils: a possible therapeutic strategy against Parkinson's disease. *Biochemistry* 2003;42:3696–3700.
50. Bisaglia M, Tessari I, Pinato L, Bellanda M, Giraud S, Fasano M, Bergantino E, Bubacco L, Mammì S. A topological model of the interaction between  $\alpha$ -synuclein and sodium dodecyl sulfate micelles. *Biochemistry* 2005;44:329–339.
51. Perrin RJ, Woods WS, Clayton DF, George JM. Exposure to long chain polyunsaturated fatty acids triggers rapid multimerization of synucleins. *J Biol Chem* 2001;276:41958–41962.
52. Leng Y, Chase TN, Bennett MC. Muscarinic receptor stimulation induces translocation of an  $\alpha$ -synuclein oligomer from plasma membrane to a light vesicle fraction in cytoplasm. *J Biol Chem* 2001;276:28212–28218.
53. Jo E, Fuller N, Rand RP, St. George-Hyslop P, Fraser PE. Defective membrane interactions of familial Parkinson's disease mutant A30P  $\alpha$ -synuclein. *J Mol Biol* 2002;315:799–807.
54. Jo E, Darabie AA, Han K, Tandon A, Fraser PE, McLaurin J.  $\alpha$ -Synuclein-synaptosomal membrane interactions - Implications for fibrillogenesis. *Eur J Biochem* 2004;271:3180–3189.
55. Cole NB, Murphy DD, Grider T, Rueter S, Brasaemle D, Nussbaum RL. Lipid droplet binding and oligomerization properties of the Parkinson's disease protein  $\alpha$ -synuclein. *J Biol Chem* 2002;277:6344–6352.
56. Lee HJ, Choi C, Lee S-J. Membrane-bound  $\alpha$ -synuclein has a high aggregation propensity and the ability to seed the aggregation of the cytosolic form. *J Biol Chem* 2002;277:671–678.
57. Necula M, Chirita CN, Kuret J. Rapid anionic micelle-mediated  $\alpha$ -synuclein fibrillization *in vitro*. *J Biol Chem* 2003;278:46674–46680.
58. Tsigelny IF, Bar-On P, Sharikov Y, Crews L, Hashimoto M, Miller MA, Keller SH, Platoshyn O, Yuan JX-J, Masliah E. Dynamics of  $\alpha$ -synuclein aggregation and inhibition of pore-like oligomer development by beta-synuclein. *FEBS J* 2007;274:1862–1877.
59. Ahmad F, Tangirala R, Raman B, Rao M. Fibrillogenic and non-fibrillogenic ensembles of SDS-bound human  $\alpha$ -synuclein. *J Mol Biol* 2006;364:1061–1072.
60. Brooks BR, Brucoleri RE, Olafson BD, States DJ, Swaminathan S, Karplus M. Charmm—a program for macromolecular energy, minimization, and dynamics calculations. *J Comput Chem* 1983;4:187–217.
61. Lazaridis T. Implicit solvent simulations of peptide interactions with anionic lipid membranes. *Proteins* 2005;58:518–527.
62. Lazaridis T. Effective energy function for proteins in lipid membranes. *Proteins* 2003;52:176–192.
63. Neria E, Fischer S, Karplus M. Simulation of activation free energies in molecular systems. *J Chem Phys* 1996;105:1902–1921.
64. McLaughlin S. The electrostatic properties of membranes. *Ann Rev Biophys Biophys Chem* 1989;18:113–136.
65. Mihajlovic M, Lazaridis T. Calculations of pH-dependent binding of proteins to biological membranes. *J Phys Chem B* 2006;110:3375–3384.
66. Kumar S, Bansal M. Structural and sequence characteristics of long  $\alpha$  helices in globular proteins. *Biophys J* 1996;71:1574–1586.
67. Mishra VK, Palgunachari MN, Segrest JP, Anantharamaiah GM. Interactions of synthetic peptide analogs of the class A amphipathic helix with lipids. *J Biol Chem* 1994;269:7185–7191.
68. Negro A, Brunati AM, Donella-Deana A, Massimino ML, Pinna LA. Multiple phosphorylation of  $\alpha$ -synuclein by protein tyrosine kinase Syk prevents eosin-induced aggregation. *FASEB J* 2002;16:210–212.
69. Lazaridis T, Karplus M. Effective energy function for proteins in solution. *Proteins* 1999;35:133–152.
70. Pleiss J, Jähnig F. Collective vibrations of an  $\alpha$ -helix—a molecular dynamics study. *Biophys J* 1991;59:795–804.
71. Landau LD, Lifshitz EM. *Theory of elasticity*. New York: Pergamon Press; 1970. 165p.
72. Klon AE, Jones MK, Segrest JP, Harvey SC. Molecular belt models for the apolipoprotein A-I Paris and Milano mutations. *Biophys J* 2000;79:1679–1685.
73. Lupas A. Coiled coils: new structures and new functions. *Trends Biochem Sci* 1996;21:375–382.
74. Walshaw J, Woolfson DN. SOCKET: a program for identifying and analysing coiled-coil motifs within protein structures. *J Mol Biol* 2001;307:1427–1450.
75. May S, Harries D, Ben-Shaul A. Lipid demixing and protein-protein interactions in the adsorption of charged proteins on mixed membranes. *Biophys J* 2000;79:1747–1760.
76. Tzllil S, Ben-Shaul A. Flexible charged macromolecules on mixed fluid lipid membranes: theory and Monte Carlo simulations. *Biophys J* 2005;89:2972–2987.
77. Madine J, Doig AJ, Middleton DA. A study of the regional effects of  $\alpha$ -synuclein on the organization and stability of phospholipid bilayers. *Biochemistry* 2006;45:5783–5792.
78. Gazzara JA, Phillips MC, Lund-Katz S, Palgunachari MN, Segrest JP, Anantharamaiah GM, Rodriguez WV, Snow JW. Effect of vesicle size on their interaction with class A amphipathic helical peptides. *J Lipid Res* 1997;38:2147–2154.
79. Wieprecht T, Apostolov O, Seelig J. Binding of the antibacterial peptide magainin 2 amide to small and large unilamellar vesicles. *Biophys Chem* 2000;85:187–198.
80. Wieprecht T, Beyermann M, Seelig J. Thermodynamics of the coil- $\alpha$ -helix transition of amphipathic peptides in a membrane environment: the role of vesicle curvature. *Biophys Chem* 2002;96:191–201.

81. Chenal A, Vernier G, Savarin P, Bushmarina NA, Gèze A, Guillain F, Gillet D, Forge V. Conformational states and thermodynamics of  $\alpha$ -lactalbumin bound to membranes: a case study of the effects of pH, calcium, lipid membrane curvature and charge. *J Mol Biol* 2005;349:890–905.
82. Edholm O, Jähnig F. The structure of a membrane-spanning polypeptide studied by molecular dynamics. *Biophys Chem* 1988;30:279–292.
83. Van Buuren AR, Berendsen HJC. Molecular dynamics simulation of the stability of a 22-residue  $\alpha$ -helix in water and 30% trifluoroethanol. *Biopolymers* 1993;33:1159–1166.
84. Shen L, Bassolino D, Stouch T. Transmembrane helix structure, dynamics, and interactions: multi-nanosecond molecular dynamics simulations. *Biophys J* 1997;73:3–20.
85. Zagrovic B, Jayachandran G, Millett IS, Doniach S, Pande VS. How large is an  $\alpha$ -helix? Studies of the radii of gyration of helical peptides by small-angle X-ray scattering and molecular dynamics. *J Mol Biol* 2005;353:232–241.
86. Knight JD, Hebda JA, Miranker AD. Conserved and cooperative assembly of membrane-bound  $\alpha$ -helical states of islet amyloid polypeptide. *Biochemistry* 2006;45:9496–9508.
87. Kirkitadze MD, Condron MM, Teplow DB. Identification and characterization of key kinetic intermediates in amyloid  $\beta$ -protein fibrillogenesis. *J Mol Biol* 2001;312:1103–1119.
88. Bouchard M, Zurdo J, Nettleton EJ, Dobson CM, Robinson CV. Formation of insulin amyloid fibrils followed by FTIR simultaneously with CD and electron microscopy. *Protein Sci* 2000;9:1960–1967.
89. Fezoui Y, Hartley DM, Walsh DM, Selkoe DJ, Osterhout JJ, Teplow DB. A de novo designed helix-turn-helix peptide forms nontoxic amyloid fibrils. *Nat Struct Biol* 2000;7:1095–1099.
90. Zhu M, Souillac PO, Ionescu-Zanetti C, Carter SA, Fink AL. Surface-catalyzed amyloid fibril formation. *J Biol Chem* 2002;277: 50914–50922.